Toward the Ultimate Conservative Scheme: Following the Quest

R. Abgrall

Mathématiques Appliquées de Bordeaux, Université Bordeaux I, 351 Cours de la Libération,
33 405 Talence Cedex, France
E-mail: abgrall@math.u-bordeaux.fr

The aim of this paper is to develop a class of numerical schemes that work on triangular finite element type meshes, and which are devoted to the computation of steady transonic flows. The schemes are extensions of the positive streamwise invariant scheme of Struijs and are built directly on the system of the Euler equation for fluid mechanics. They are a blending between a first-order and a second-order scheme, which is realized from entropy considerations. It is formally second-order accurate at steady state. Several numerical examples are shown to demonstrate the stability and accuracy of these schemes. ©️ 2001 Academic Press

Key Words: compressible flow solvers; residual schemes; fluctuation splitting schemes; unstructured meshes; multidimensional up-winding.

1. INTRODUCTION

We are interested in the numerical approximation of the Euler equations of fluid mechanics in a domain Ω with boundary conditions,

$$
\begin{aligned}
&\frac{\partial W}{\partial t} + \operatorname{div} \mathcal{F}(W) = 0 \quad t > 0 \text{ and } x \in \Omega \\
&W(x, 0) = W_0(x) \qquad x \in \Omega \\
&\text{boundary conditions} \quad \text{on } \partial\Omega.
\end{aligned}
\tag{1}
$$

The flux $\mathcal{F} = (F, G)$ and the conserved variables are given by

$$
W = (\rho, \rho u, \rho v, E)^T, \quad F(W) = (\rho u, \rho u^2 + p, \rho uv, u(E + p))^T,
$$

$$
G(W) = (\rho v, \rho uv, \rho v^2 + p, v(E + p))^T,
$$

where ρ is the density, u and v are the components of the velocity, ϵ is the internal energy, and $E = \rho\epsilon + \frac{1}{2}\rho(u^2 + v^2)$ is the total energy. The system is closed by the equation of

277

state relating the pressure p to the conserved variables,

$$p = (\gamma - 1)\left(E - \frac{1}{2}\rho(u^2 + v^2)\right) = (\gamma - 1)\rho\epsilon.$$

The ratio of specific heats γ is kept constant; $\gamma = 1.4$ in the applications.

The system (1) has to be supplemented by the entropy inequality which translates the second law of thermodynamics,

$$\frac{\partial S}{\partial t} + \frac{\partial(uS)}{\partial x} + \frac{\partial(vS)}{\partial y} \leq 0 \quad \text{on } \Omega. \tag{2}$$

Here, the mathematical entropy is given by $S = -\rho h(s)$ [9], where s is the physical entropy

$$s = c_v \log\left(\frac{p}{\rho^\gamma}\right) + s_0 \tag{3}$$

and h is any real-valued function such that

$$h' > 0 \quad \text{and} \quad \frac{h''}{h'} < \gamma^{-1}.$$

In the practical examples, we take $h(x) = x$. If the flow is smooth, (3) is equivalent to

$$\frac{\partial s}{\partial t} + u\frac{\partial s}{\partial x} + v\frac{\partial s}{\partial y} = 0 \quad (\geq 0) \tag{4}$$

and Tadmor has shown [14] that the solution (if it is bounded) adheres to the minimum principle

$$s(x, t) \geq \min_{\|y - x\| \leq t\|\mathbf{u}\|_\infty} s(y, 0), \tag{5}$$

where $\|x\|$ is the Euclidean norm of x and $\|\mathbf{u}\|_\infty$ is the L^∞ norm of the velocity field.

In this paper, we are mainly interested in computing the steady solution of (1). This task has become a routine in many modern CFD codes. Many current schemes use ideas for high-resolution schemes developed in the 1970s and 1980s by van Leer, Roe, Osher, Harten, Yee, Sweby, and many others. The list is enormous, and some of the most significant contributions have been collected in [10]. However, the quality of the solution is still questionable: some apparently simple problems, such as computing the lift and drag of an airfoil, still pose difficulty. One reason is that the so-called high-resolution schemes suffer a much too great entropy production. In fact, they have been devised on scalar 1D problems, then extended to multiD systems; but their construction relies on "1D ideas." Another difficult problem is the sensitivity to the mesh. It is still difficult to construct a 3D mesh of good quality and, consequently, the quality of the solution itself may be questionable in many cases. Hence, it is natural to try to develop methods that have as little sensitivity as possible to the regularity of the mesh.

For these reasons, for several years, researchers have tried to incorporate ideas contained in the 1D high-resolution schemes (upwind) into a finite-element-like framework. Some of the major contributions have been made by P. L. Roe, H. Deconinck, D. Sidilkover, and their coauthors. These fluctuation splitting schemes, were first developed for a scalar transport

equation, then formally extended to the system (see [6, 13] for example) by incorporating as much physics as possible. These schemes share many common features with the SUPG scheme of Hughes or the streamline diffusion methods of Johnson, except for up-winding. These schemes are not constructed by deeply using any particular direction of the mesh. One advantage is that, at least for scalar equations, one can construct a fully second-order-accurate scheme on triangular meshes with a very compact stencil; the scheme uses only the neighboring nodes.

In our opinion, the maturity of these new schemes is still not sufficient: they may lack robustness, the formulation may not be simple enough, etc. The aim of the present paper is to give some elements that might clarify the construction of second-order upwind residual schemes.

We first give some generalities on fluctuation splitting schemes. In particular, we connect them to finite volume schemes and show why they offer more flexibility. We recall Roe–Struijs–Deconinck linearization [5], give a simple condition that guarantees a Lax–Wendroff-like theorem, and describe the design principle of our scheme. Then, we recall two important examples of the system N (narrow) and the LDA (low diffusion advection) system schemes introduced by van der Weide and Deconinck [15] after their scalar version. We show they are well defined for a symetrizable system. Barth [2, 4] has shown that for a linear symetrizable system the N scheme is globally and locally dissipative. In the next section, we give a different interpretation of the PSI (Positive Stream Wise Invariant) scheme, and we show how to extend it to (1). Last, we give numerical examples to illustrate the scheme.

2. THE FLUCTUATION SPLITTING SCHEMES

2.1. *Generalities*

Throughout the paper, we consider a two-dimensional computational domain Ω that is triangulated. For the moment, we forget the boundary conditions. The set of triangles is $\{T_j\}_{j=1,\ldots,nt}$. The mesh points are $\{M_i\}_{i=1,\ldots,n_s}$. The vertices of a triangle T are M_{i_1}, M_{i_2}, M_{i_3}. When there is no ambiguity, they are denoted by their index in the list $\{M_i\}_{i=1,\ldots,n_s}$, namely i_1, i_2, i_3, or simply by 1, 2, 3. To discretize (1), we consider the following residual scheme:

$$|C_i| \frac{W_i^{n+1} - W_i^n}{\Delta t} + \sum_{T, M_i \in T} \Phi_i^T = 0. \tag{6}$$

In this equation, W_i^n is an approximation of $W(M_i, t_n)$, $|C_i|$ is the area of the dual control volume (see Fig. 1), and the residuals Φ_i^T are function of W_i^n and its neighboring values. The residuals are assumed to fulfill the condition

$$\sum_{M_i \in T} \Phi_i^T = \int_T \operatorname{div} \mathcal{F}^h \, dx \text{ for any triangle } T, \tag{7}$$

where $\mathcal{F}^h$ is an approximation of $\mathcal{F}$. In [3], it is shown that under reasonable assumptions on the Φ_i^T's (continuity, convergence of $\mathcal{F}^h$ toward $\mathcal{F}$, continuity of $\mathcal{F}^h$ on the edges of T) and the classical assumption of the Lax–Wendroff theorem [11], the numerical solution converges to a weak solution of (1).
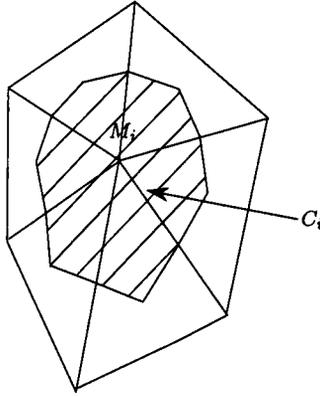
FIG. 1. The dual cell is obtained by joining the midpoints of the edges starting from M_i and the centroids of the triangles containing M_i as a vertex.

An example is given by the following finite-volume scheme (see Fig. 2 for the notations). The numerical flux on the edge $[M_i, M_j]$ is

$$F(W_i, W_j, \mathbf{n}_{ij}) = \frac{1}{2}\left(\mathcal{F} \cdot \mathbf{n}_{ij}^1(W_j) + \mathcal{F} \cdot \mathbf{n}_{ij}^1(W_i) - Q\left(W_i, W_j, \mathbf{n}_{ij}^1\right) \cdot (W_i - W_j)\right)$$
$$+ \frac{1}{2}\left(\mathcal{F} \cdot \mathbf{n}_{ij}^2(W_j) + \mathcal{F} \cdot \mathbf{n}_{ij}^2(W_i) - Q\left(W_i, W_j, \mathbf{n}_{ij}^2\right) \cdot (W_i - W_j)\right). \quad (8)$$

In (8), we have used the notation $\mathcal{F} \cdot \mathbf{n}$ for $n_x F(W) + n_y G(W)$, where n_x and n_y are the two components of $\mathbf{n}$. Since the boundary of C_i is closed, the scheme would be the same if we had set

$$\Phi_i^{T_1} = \frac{1}{2}\left(\mathcal{F} \cdot \mathbf{n}_{ij}^1(W_j) - \mathcal{F} \cdot \mathbf{n}_{ij}^1(W_i) - Q\left(W_i, W_j, \mathbf{n}_{ij}^1\right) \cdot (W_i - W_j)\right)$$
$$+ \frac{1}{2}\left(\mathcal{F} \cdot \mathbf{n}_{ik}^1(W_k) - \mathcal{F} \cdot \mathbf{n}_{ik}^1(W_i) - Q\left(W_i, W_k, \mathbf{n}_{ik}^1\right) \cdot (W_i - W_k)\right) \quad (9)$$

and the same for T_2. In Eq. (9), the indices j and k denote the indices of the two vertices of
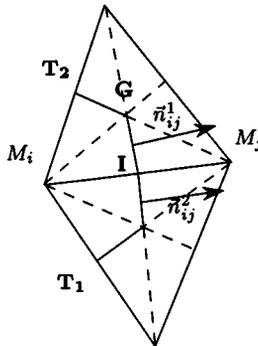

FIG. 2. Geometrical elements for the finite volume scheme. The normal $\mathbf{n}_{ij}^1$ is orthogonal to $[G, I]$ with the same length. Same for $\mathbf{n}_{ij}^2$.

T_1 different from M_i. In the end, we get

$$\sum_{M_i \in T_1} \Phi_i^{T_1} = \frac{1}{2} \sum_{M_i \in T_1} \mathcal{F}(W_i) \cdot \mathbf{n}_i,$$

where $\mathbf{n}_j$ is the inward normal of T_1 opposite to the node M_j. Here, the approximation $\mathcal{F}^h$ is the piecewise linear interpolant of the flux.

Other schemes that cast immediately into this formulation are the finite-element-like schemes, i.e., the SUPG schemes and the streamline diffusion method.

The main advantage of the residual formulation is that we are no longer constrained by the geometry of the mesh, as in the finite volume schemes. Only relation (7) and the continuity of $\mathcal{F}^h$ through the edges are important; hence much more flexibility is possible.

2.2. The Roe–Struijs–Deconinck Linearization

The parameter vector is given by

$$Z = (\sqrt{\rho}, \sqrt{\rho}u, \sqrt{\rho}v, \sqrt{\rho}H)^T = (z_1, z_2, z_3, z_4)^T,$$

where $H = \frac{E+p}{\rho}$ is the enthalpy. Note that $W = W(Z)$ and $\mathcal{F} = \mathcal{F}(Z)$ are quadratic in Z,

$$W(Z) = \frac{1}{2} D(Z)Z, \quad \mathcal{F}(Z) = \frac{1}{2} \mathcal{R}(Z) \cdot Z, \tag{10}$$

where $D(Z)$ and $\mathcal{R}(Z)$ are matrices that depend linearly on Z. The matrix $D(Z)$ is a triangular matrix and is invertible as soon as $z_1 \neq 0$. The matrices D and $\mathcal{R}$ have been chosen to be the Jacobian matrices of W (resp. $\mathcal{F}$) with respect to Z.

If Z is linearly interpolated on T by Z^h, we set

$$\mathcal{F}^h(x, y) = \mathcal{F}(Z^h)$$

and simple calculations show that

$$\int_T \operatorname{div} \mathcal{F}^h(x, y)\, dx\, dy = \int_T \bar{A} \frac{\partial W^h}{\partial x} + \bar{B} \frac{\partial W^h}{\partial y}\, dx\, dy,$$

where

$$\bar{A} = \frac{\partial F}{\partial W}(W(\bar{Z})), \quad \bar{B} = \frac{\partial G}{\partial W}(W(\bar{Z})) \quad \text{with } \bar{Z} = \frac{Z_1 + Z_2 + Z_3}{3}. \tag{11}$$

More explicitly, we have

$$(\bar{A}, \bar{B}) = \mathcal{R}(\bar{Z}) D^{-1}(\bar{Z}).$$

Since the Jacobian matrices are functions of the velocity and the enthalpy only, the matrices

$\bar{A}$ and $\bar{B}$ are functions of

$$\bar{u} = \frac{\sqrt{\rho_1}u_1 + \sqrt{\rho_2}u_2 + \sqrt{\rho_3}u_3}{\sqrt{\rho_1} + \sqrt{\rho_2} + \sqrt{\rho_3}},$$

$$\bar{v} = \frac{\sqrt{\rho_1}v_1 + \sqrt{\rho_2}v_2 + \sqrt{\rho_3}v_3}{\sqrt{\rho_1} + \sqrt{\rho_2} + \sqrt{\rho_3}}, \tag{12}$$

$$\bar{H} = \frac{\sqrt{\rho_1}H_1 + \sqrt{\rho_2}H_2 + \sqrt{\rho_3}H_3}{\sqrt{\rho_1} + \sqrt{\rho_2} + \sqrt{\rho_3}}.$$

In the following we set

$$K_i = \frac{1}{2}\left(\bar{A}n_x^i + \bar{B}n_y^i\right),$$

where n_x^i, n_y^i are the components of the outward unit vector $\mathbf{n}_i$ of the side of T opposite to M_i.

One of the important properties of the linearization is that the matrices K_i are easy to compute, and they are diagonalizable, with real eigenvalues.

The eigenvalues of K_i are $\lambda = u_n \pm c, u_n, u_n$. Hence, to show that the matrices K_i always have real eigenvalues, because of Eq. (11), it is enough to show that the average speed of sound defined by

$$\frac{\bar{c}^2}{\gamma - 1} = \bar{H} - \frac{1}{2}(\bar{u}^2 + \bar{v}^2) = \bar{h} + \delta,$$

where $\bar{h}$ stands for the average specific enthalpy with the same weight coefficients as in (12), is a real number. The rest δ is quadratic in speed and is given by

$$\delta(\sqrt{\rho_1} + \sqrt{\rho_2} + \sqrt{\rho_3})^2 = (u_1, u_2, u_3)P(u_1, u_2, u_3)^T + (v_1, v_2, v_3)P(v_1, v_2, v_3)^T.$$

If $z_1 = \sqrt{\rho_1}$, etc., we get

$$P = \begin{pmatrix} z_1(z_2 + z_3) & -z_1 z_2 & -z_1 z_3 \\ -z_1 z_2 & z_2(z_1 + z_3) & -z_3 z_1 \\ -z_1 z_3 & -z_3 z_2 & z_3(z_1 + z_2) \end{pmatrix}.$$

This matrix is symmetric and positive because its eigenvalues are

$$\lambda_1 = 0, \quad \lambda_2 = \nu + \eta, \quad \lambda_3 = \nu - \eta$$

with

$$\nu = z_1 z_2 + z_1 z_3 + z_3 z_2$$

$$\eta^2 = z_1^2 z_2^2 + z_1^2 z_3^2 + z_2^2 z_3^2 - z_1^2 z_2 z_3 - z_1 z_2^2 z_3 - z_3^2 z_2 z_1.$$

We can see that $\eta^2 = (z_1 z_2 + z_1 z_3 + z_2 z_3)^2 - 3z_1 z_2 z_3(z_1 + z_2 + z_3)$ is always positive. If we left z_2 and z_3 constant, η^2 becomes a second-degree polynomial for which the discriminant $-3z_3^2 z_2^2(z_2 - z_3)^2$ is negative. The coefficient η^2 thus has a constant sign, positive. Moreover, $\eta^2 \leq z_1^2 z_2^2 + z_1^2 z_3^2 + z_2^2 z_3^2 \leq (z_1 z_2 + z_1 z_3 + z_2 z_3)^2$, so all the eigenvalues of P are positive. Thus, $\delta \geq 0$ and $\bar{c}^2 \geq 0$. Hence we get

PROPOSITION 2.1. *If the densities ρ_i are positive, the Roe–Struijs–Deconinck's linearization is diagonalizable with real eigenvalue matrices K_i.*

Note that the conservation relation (7) reads

$$\Phi^T = \sum_{M_i \in T} K_i Z_i, \tag{13}$$

where K_i is computed via the Jacobian of the fluxes with respect to Z.

3. DESIGN PRINCIPLES

In this section, we present three design principles (up-winding, the linear preserving property, and a monotonicity condition) and give some examples.

3.1. *The Up-Winding Property*

Following Roe, Deconinck *et al.*, [6] we have that the scheme is upwind if the following condition is true:

($\mathcal{U}$) if all the eigenvalues of K_i are negative, then $\Phi_i^T = 0$.

3.2. *Second-Order Accuracy at Steady State: The Linear Preserving Condition (LP)*

At steady state, scheme (6) satisfies

$$\text{for any node } M_i, \ \sum_{T, M_i \in T} \Phi_i^T = 0.$$

For any smooth function $\varphi \in C^1(\mathbb{R}^4)^4$, we have

$$\sum_{M_i} \varphi_i \cdot \left(\sum_{T, M_i \in T} \Phi_i^T \right) = 0.$$

Setting $\varphi_G^T = (\varphi_1 + \varphi_2 + \varphi_3)/3$, the value of the piecewise linear interpolant of φ at the centroid of T, we have, after having used (7),

$$\sum_T \varphi_G^T \int_T \operatorname{div} \mathcal{F}^h \, dx \, dy + \sum_T \sum_{M_i \in T} \left(\varphi_i - \varphi_G^T \right) \cdot \Phi_i^T = 0. \tag{14}$$

To get second-order accuracy at steady state, the second term of equation [14] must be of the form

$$\sum_{M_i} \left(\varphi_i - \varphi_G^T \right) \cdot \left(\sum_{T, M_i \in T} \Phi_i^T \right) = \mathcal{O}(h^2) \tag{15}$$

when the arguments of the residuals are replaced by a smooth solution of (1). In (15), h is the maximum diameter of the triangles T.

One way of ensuring this condition is, for any smooth solution W of (1), to have $\Phi_i^T(W) = \mathcal{O}(h^3)$ because of (14). This is clear from (14) because (a) the number of vertices in a bounded

domain is $\mathcal{O}(h^{-2})$ for a regular mesh and (b) Eq. (15) requires that $(\varphi_i - \varphi_C)\Phi_i^T = \mathcal{O}(h^4)$ which is true since $\varphi_i - \varphi_G = \mathcal{O}(h)$.

This condition is obtained for the SUPG and streamline diffusion schemes because the residual is written

$$\Phi_i^T = \beta_i^T \Phi^T$$

with β_i^T uniformly bounded independent of the mesh. For a smooth solution of the steady version of (1), one has $\Phi^T = \int_T \operatorname{div} \mathcal{F}^h(W) \, dx = \mathcal{O}(h^3)$. Indeed, we have

$$\int_T \operatorname{div} \mathcal{F}^h(W) \, dx = \int_T \operatorname{div}(\mathcal{F}^h(W) - \mathcal{F}(W)) \, dx$$

$$= \int_{\partial T} (\mathcal{F}^h(W) - \mathcal{F}(W)) \cdot \mathbf{n} \, dl.$$

Assuming that $\mathcal{F}^h$ is a second-order approximation of $\mathcal{F}$, and since the length of ∂T is $\mathcal{O}(h)$, we get

$$\Phi^T = \int_T \operatorname{div} \mathcal{F}^h(W) \, dx = \mathcal{O}(h^3).$$

This proof makes clear two facts:

1. The scheme we construct can be second-order accurate only for steady problems.
2. The approximation $\mathcal{F}^h$ of the flux must be second-order accurate. This is true for the Roe–Deconinck–Struijs linearization.

The condition $\Phi_T = \mathcal{O}(h^3)$ is not clear, and probably untrue, for finite volume schemes, because it necessitates geometrical cancellations that are not true in general (except for very regular meshes with geometrical invariance properties).

3.3. *The Monotonicity Condition*

This condition is very clear for a scalar equation and quite intuitive but difficult to formalize for a system. The idea is to have a condition that avoids the creation of unphysical oscillations. For a scalar equation, this condition is met, up to a CFL-like condition, if the residual sent at node M_i has the structure

$$\Phi_i^T = \sum_{M_j \in T} c_{ij}(u_i - u_j)$$

with $c_{ij} \geq 0$ and uniformly bounded. These schemes are L^∞ stable under a CFL condition.

In the case of a system, this monotonicity condition is meaningless, but one still wants to avoid unphysical oscillations. Some well-considered schemes admit unphysical solutions, such as the ENO schemes [1], but the constraints are such that one can reasonably expect that these oscillations are weak and vanish when the mesh size tends to zero; and this is indeed the case in practice.

When a monotonicity condition exists, the scheme is L^∞ stable. In this paper, we replace a monotonicity condition by a formal approximation of the inequality (4). If (4) were numerically true, we would have a discrete version of (5) (under a CFL condition) and since s is concave, the scheme would be L^∞ stable.

4. EXAMPLES

We give two examples of upwind schemes: the system N scheme and the system LDA scheme of Deconinck and van der Weide [15].

4.1. *The System N Scheme*

We set

$$\Phi_i^T = K_i^+(\tilde{W}_i - \tilde{W}), \tag{16}$$

where $K_i = \bar{A}n_x^i + \bar{B}n_y^i$ and $\tilde{W}_i = D(\bar{Z})Z_i$.[1] In order to recover the conservation relation (13), we must have

$$\left(\sum_{i=1,3} K_i^-\right)\tilde{W} = \sum_{i=1,3} K_i^-\tilde{W}_i. \tag{17}$$

To define $\tilde{W}$, one has a priori to invert the matrix

$$\sum_{i=1,3} K_i^-,$$

which in some cases, may be impossible. When it is possible, we denote by N the matrix

$$N = \left(\sum_{i=1,3} K_i^-\right)^{-1}. \tag{18}$$

However, we show in Appendix B that, for the Euler equations, $K_i^+\tilde{W}$ is always defined. More precisely, we show that for the scalar product $\langle .\,,.\rangle$ defined by A_0, the Hessian of the mathematical entropy S evaluated at the same average state that is used to define $\bar{A}$ and $\bar{B}$, the space of state $\mathbb{R}^4$ can be written as

$$\mathbb{R}^4 = \mathbb{R}r_0 \oplus H,$$

where

$$r_0 = \begin{pmatrix} 1 \\ \bar{u} \\ \bar{v} \\ \frac{1}{2}(\bar{u}^2 + \bar{v}^2) \end{pmatrix}.$$

The space H is the orthogonal complement of $r_0\mathbb{R}$ for $\langle .\,,.\rangle$. The projector onto H is given by

$$\pi(W) = W - \frac{\langle W, v_0 \rangle}{\langle r_0, v_0 \rangle}r_0. \tag{19}$$

---

[1] If K is a diagonalizable matrix with real eigenvalues ($K = L\Lambda R$) $\Lambda = \mathrm{diag}(\lambda)$, then $K^{\pm} = L\Lambda^{\pm}R$ where $\Lambda^{\pm} = \mathrm{diag}(\lambda^{\pm})$.

The vector v_0 is $\nabla_W s$ evaluated at the average state; it is the (common) left eigenvector of $\bar{A}$ and $\bar{B}$. We also denote by $\pi^\perp$ the projector

$$\pi^\perp(W) = \frac{\langle W, v_0 \rangle}{\langle r_0, v_0 \rangle} r_0. \tag{20}$$

It gives the component of W along the entropy wave. The adjoint π^* of π is given by

$$\pi^*(W) = W - \frac{\langle W, r_0 \rangle}{\langle r_0, v_0 \rangle} v_0 \tag{21}$$

and satisfies $A_0\pi = \pi^* A_0$.

We can give a meaning to the inverse of $\sum_{i=1,3} K_i^-$, denoted by N. The proof is valid for a linearized symmetric system and is given in Appendix B.

The N scheme is linearly dissipative when the system is symetrizable. More precisely, if the linearization is carried out in the entropy variables V, T. Barth [2, 4] has shown that

LEMMA 4.1. *If the matrices K_i are symmetric, one has*

$$\sum_{M_i \in T} \langle V_i, \Phi_i^T \rangle = \frac{1}{2} \sum_{M_i \in T} \langle V_i, K_i V_i \rangle + \mathcal{Q}_N(V_1, V_2, V_3), \tag{22}$$

where

$$2\mathcal{Q}_N(V_1, V_2, V_3) = -\langle \Phi^T N, \Phi^T \rangle + \sum_{M_i \in T} (\langle V_i, K_i^+ V_i \rangle - \langle K_i^+ V_i, N K_i^+ V_i \rangle)$$

$$+ \sum_{M_i \in T} (\langle V_i, -K_i^- V_i \rangle - \langle -K_i^+ V_i, N(-K_i^-)V_i \rangle). \tag{23}$$

The quadratic form $\mathcal{Q}_N$ is positive: the N scheme is locally dissipative.

He shows that *each* of the three terms in (23) is positive. The proof of Lemma 4.1 is reproduced in Appendix A.

In the case of a linear problem, the sum of $\langle V_i, K_i V_i \rangle$ cancels, and we get a *global* energy stability result for the N scheme. If we had a linearization in the *entropy variable* $V = \nabla_W S$, we could interpret $\frac{1}{2}\sum_{M_i \in T} \langle V_i, K_i V_i \rangle$ as

$$\int_{\partial T} \langle V, K_n V \rangle^h \, d\sigma,$$

where the "energy" $\langle V, K_n V \rangle$ is piecewise linearly interpolated by $\langle V, K_n V \rangle^h$. Hence, using exactly the same technique as in [3], if the conditions of the Lax–Wendroff theorem are true, then the limit of the numerical solutions satisfies an entropy inequality, namely

$$\frac{\partial S}{\partial t} + \operatorname{div}(uS) \le 0.$$

4.2. *The System LDA Scheme*

The straightforward extension of the scalar LDA scheme is given by

$$\Phi_i^T = -K_i^+ N \Phi^T, \tag{24}$$

where the N matrix is given by (18). The conservation relation is obviously satisfied. This scheme is upwind and LP.

When the linearization is carried out in the entropy variables, and if we set

$$V^+ = -N\left(\sum_{i=1,3} K_i^+ V_i\right) \quad \text{and} \quad V^- = N\left(\sum_{i=1,3} K_i^- V_i\right),$$

we have

$$\sum_{M_i \in T} \langle V_i, \Phi_i^T \rangle = \frac{1}{2} \sum_{M_i \in T} \langle V_i, K_i V_i \rangle + \mathcal{Q}_{LDA}(V_1, V_2, V_3) \tag{25}$$

with

$$\begin{aligned}
2\mathcal{Q}_{\mathrm{LDA}}(V_1, V_2, V_3) = & \sum_{i=1}^{3} \langle V^+ - \tilde{V}_i, K_i^+(V^+ - \tilde{V}_i) \rangle + \sum_{i=1}^{3} \langle \tilde{V}_i - V^-, K_i^+(\tilde{V}_i - V^-) \rangle \\
& + \sum_{M_i \in T} \left(\langle V_i, K_i^+ V_i \rangle + \langle K_i^+ V_i, N K_i^+ V_i \rangle \right) \\
& + \sum_{M_i \in T} \left(\langle V_i, -K_i^- V_i \rangle + \langle -K_i^+ V_i, N(-K_i^-) V_i \rangle \right).
\end{aligned} \tag{26}$$

Unfortunately, $\mathcal{Q}_{\mathrm{LDA}}$ is not a positive quadratic form.

4.3. *Additional Properties of the LDA and N Schemes*

It is also possible to compare $\mathcal{Q}_N$ and $\mathcal{Q}_{\mathrm{LDA}}$ for a symetrizable system when the linearization is done via the entropy variables.

LEMMA 4.2.   *We have*

$$\mathcal{Q}_{\mathrm{LDA}}(V_1, V_2, V_3) \le \mathcal{Q}_N(V_1, V_2, V_3).$$

This result states that the N scheme is more dissipative than the LDA scheme. We have the following additional property.

LEMMA 4.3.

1. *If Φ_i is the residual for the N scheme or the LDA scheme, we have*

$$\langle V, \pi \Phi_i(V_1, V_2, V_3) \rangle = \langle \pi^* V, \Phi_i(\pi^* V_1, \pi^* V_2, \pi^* V_3) \rangle.$$

2. *The results of Lemmas 4.1 and 4.2 are valid on H and $\mathbb{R} r_0$.*

This result states that we can split the energy contribution of the residuals into their contributions along the entropy wave and its orthogonal complement.

5. AN LP POSITIVE SCALAR SCHEME

In this section, we consider a scalar equation

$$\frac{\partial u}{\partial t} + \langle \boldsymbol{\lambda}, \nabla u \rangle = 0. \tag{27}$$

Let us first describe in detail the N and LDA schemes on a triangle T. We set $k_j = \frac{1}{2}\langle \lambda, \mathbf{n}_i \rangle$. Since $\sum_{j=1}^{3} k_j = 0$, there are two generic cases: Either only one of the k_j is strictly positive, or two of them are strictly positive. The first case is called the "one-target case," the second one the "two-target case." For the sake of simplicity, let us assume that $k_1 > 0$, and $k_2 > 0$ in the two-target case. We have

- One-target case:

$$\Phi_1^N = \Phi$$
$$\Phi_2^N = 0$$
$$\Phi_3^N = 0.$$

Since $-k_2 \geq 0$ and $-k_3 \geq 0$, the scheme is positive if

$$\Delt \frac{\sum_{k_j \geq 0} k_j}{|C_i|} \leq 1.$$

- Two-target case:

$$\Phi_1^N = k_1(u_1 - u_3)$$
$$\Phi_2^N = k_2(u_2 - u_3)$$
$$\Phi_3^N = 0.$$

Since $k_1 \geq 0$ and $k_2 \geq 0$, the scheme is positive if

$$\Delta t \frac{\sum_{k_j \geq 0} k_j}{|C_i|} \leq 1.$$

The condition $\Delta t \sum_{k_j \geq 0} |k_j|/|C_i| \leq 1$ is a global positivity condition. Similarly, the LDA scheme reads

- One-target case:

$$\Phi_1^{LDA} = \Phi = -k_2(u_1 - u_2) - k_3(u_1 - u_3)$$
$$\Phi_2^{LDA} = 0$$
$$\Phi_3^{LDA} = 0.$$

Since $-k_2 \geq 0$ and $-k_3 \geq 0$, the scheme is positive.

- Two-target case:

$$\Phi_1^{LDA} = -\frac{k_1}{k_3}\Phi$$

$$\Phi_2^{LDA} = -\frac{k_2}{k_3}\Phi$$

$$\Phi_3^{LDA} = 0.$$

In this section, we consider a scheme that is a blending between the N scheme and the LDA scheme. On any triangle T, the residual is written

$$\Phi_i = l\Phi_i^N + (1-l)\Phi_i^{LDA}.$$

We look for $l \in \mathbb{R}$ such that the scheme is positive and LP. The conservation constraints, as well as the upwind constraints, are automatically satisfied. The problem is to compute l. For this, we follow Sidilkover's technique [12],

$$\Phi_i = l\Phi_i^N + (1-l)\Phi_i^{LDA} = (l + (1-l)r_i)\,\Phi_i^N, \tag{28}$$

where $r_i = \Phi_i^{LDA}/\Phi_i^N$.

One-target case. Any value of l works since $\Phi_i^N = \Phi_i^{LDA}$ for any i. We set $l = 1$ in that case.

Two-target case. We have the relations (28) for $i = 1, 2$. Since the N scheme is positive (with a CFL constraint), the blended scheme may also be positive if

$$l + (1-l)r_1 = l(1-r_1) + r_1 \geq 0$$
$$l + (1-l)r_2 = l(1-r_2) + r_2 \geq 0. \tag{29}$$

We can write

$$\Phi_1^{LDA} = \alpha\Phi = \alpha\left(\Phi_1^N + \Phi_2^N\right)$$
$$\Phi_2^{LDA} = \beta\Phi = \beta\left(\Phi_1^N + \Phi_2^N\right)$$

with $\alpha = -\frac{k_1}{k_3} \in [0, 1]$ and $\beta = -\frac{k_2}{k_3} \in [0, 1]$ and $\alpha + \beta = 1$. Setting $r = -\Phi_1^N/\Phi_2^N$, in the inequalities (29), we write

$$l(\beta + \alpha r) + \alpha(1 - r) \geq 0$$

$$l(\alpha + \beta r) + \beta(1 - r) \geq 0.$$

A solution to this set of inequalities is

$$l = \begin{cases} 1 & \text{if } r \leq 0 \\ \max\left(\frac{\alpha(r-1)}{\beta+\alpha r}, \frac{\beta(1-r)}{\alpha+\beta r}\right) & \text{else.} \end{cases} \tag{30}$$

The formulae (30) can be rewritten as

$$
l = \begin{cases}
1 & \text{if } r \leq 0 \\
\frac{\beta(1-r)}{\alpha + \beta r} & \text{if } 0 \leq r \leq 1 \\
\frac{\alpha(r-1)}{\beta + \alpha r} & \text{if } 1 \leq r
\end{cases}
$$

so that an explicit calculation of the residuals $\Phi_i = l\Phi_i^N + (1-l)\Phi_i^{LDA}$ gives

$$
\Phi_1 = \begin{cases}
\Phi_1^N & \text{if } r \leq 0 \\
\Phi & \text{if } 0 \leq r \leq 1 \\
0 & \text{if } 1 \leq r,
\end{cases}
\qquad
\Phi_2 = \begin{cases}
\Phi_2^N & \text{if } r \leq 0 \\
0 & \text{if } 0 \leq r \leq 1 \\
\Phi & \text{if } 1 \leq r,
\end{cases}
$$

which means that in the case $r \geq 0$, all the residuals are sent either to node 1 or to node 2: this is nothing else than the positive streamwise invariant (PSI) scheme.

It is also possible to rewrite the limiter l of (30) in different forms. Take $\xi \in [0, 1[$ and define φ_ξ by

$$
\varphi_\xi(x) = \begin{cases}
\frac{r}{r-1} & \text{if } r \leq \xi \\
\frac{\xi}{\xi - 1} & \text{else.}
\end{cases}
\tag{31}
$$

We also define φ_1 as the limit of φ_ξ when $\xi \to 1$,

$$
\varphi_1(x) = \begin{cases}
\frac{r}{r-1} & \text{if } r < 1 \\
-\infty & \text{else.}
\end{cases}
$$

Then we can rewrite l of (30) as

$$
\begin{aligned}
l &= \min(1, \max(\varphi_\xi(r_1), \varphi_\xi(r_2))) \\
&= \min(1, \max(\varphi_1(r_1), \varphi_1(r_2))).
\end{aligned}
\tag{32}
$$

This remark will be useful in the following.

Another choice of limiter that does not give back the scalar PSI scheme is obtained by applying the formula (32) where φ_ξ is replaced by ψ given by

$$
\psi(x) = \frac{|x|}{|x| + 1},
\tag{33}
$$

namely

$$
l = \min(1, \max(\psi(r_1), \psi(r_2))).
\tag{34}
$$

We note that limiter (32), (31), or (34) satisfies

$$
\lim_{\phi_2^N \to 0} l = 1,
$$

which ensure the continuity of the limiter function.

6. AN LP STABLE SCHEME FOR (1)

6.1. *Comments on the System N Scheme*

All the numerical experiments that have been conducted with the system N scheme indicate it is a very stable, robust, and monotonic scheme. By saying it is monotonic, we mean that however strong the discontinuities are, there are no pre- or post-discontinuity oscillations. In particular, it is a numerical fact that the physical entropy s follows the semidiscrete relation

$$|C_i|\left(\frac{ds}{dt}\right)_i + \sum_{T,M_i\in T}\sum_{M_j\in T} c_{ij}^T(s_i - s_j) \geq 0 \tag{35}$$

for some positive numbers c_{ij}.

Since r_0 is a common eigenvector of $\bar{A}$ and $\bar{B}$, we have

$$\left\langle v_i\pi^\perp\Phi_i^{N,T}\right\rangle = \sum_{M_j\in T} c_{ij}^T\langle v_i, \pi^\perp(W_i - W_j)\rangle, \tag{36}$$

where the c_{ij}^T are the coefficients for the scalar N scheme where $\lambda = \bar{\mathbf{u}}$; i.e.,

$$k_j = \frac{1}{2}\langle\bar{\mathbf{u}}, \mathbf{n}_j\rangle,$$

$$c_{ij}^T = \frac{k_i^+ k_j^-}{\sum_{j=1,3} k_j^-}.$$

Equation (36) states that the system N scheme is positive on the (linearized) entropy wave.

Throughout the paper, we assume that a similar relation does exist on the shear and acoustic wave modes; more precisely, we assume that a relationship of the type

$$\left\langle v_i, \pi\Phi_i^{N,T}\right\rangle \leq \sum_{M_j\in T} c_{ij}^T\langle v_i, \pi(W_i - W_j)\rangle \tag{37}$$

holds even if we have been unable to prove it. The first inequality (36) states a monotonic behavior of the projection of Φ_i^T on the entropy wave. The second inequality (37) states the same for the projection of Φ_i^T on the acoustic and shear modes.

6.2. *Construction of an Entropy Stable LP Scheme*

In the following analysis, we set

$$v_i = \nabla_W s(W_i)$$

and we consider the semidiscrete scheme

$$|C_i|\left(\frac{dW}{dt}\right)_i + \sum_{T,M_i\in T}\Phi_i^T = 0,$$

where

$$\Phi_i^T = \ell\Phi_i^{N,T} + (\mathbf{Id} - \ell)\Phi_i^{LDA,T}. \tag{38}$$

Here ℓ is a matrix the structure of which has to be defined to get a monotonic entropy stable scheme.

We first left multiply $(dW/dt)_i$ by v_i, and we get

$$|C_i| \left(\frac{ds}{dt} \right)_i + \sum_{T, M_i \in T} \langle v_i, \Phi_i^T \rangle = 0.$$

The idea is to construct ℓ in such a way that

$$\frac{\langle v_i, \Phi_i^T \rangle}{\langle v_i, \Phi_i^{N,T} \rangle} \geq 0. \tag{39}$$

If it is possible, by combining this inequality with (36) and (37), provided that $\langle v_i \Phi_i^T \rangle / \langle v_i \Phi_i^{N,T} \rangle$ is bounded, we recover formally a bound on the solution, under a CFL-like condition. Now we show how it is possible to construct such a matrix ℓ.

To begin with, recall the decomposition of the state space $\mathbb{R}^4 = \mathbb{R} r_0 \oplus H$ given, for any state $W \in \mathbb{R}^4$, by

$$W = \pi(W) + \pi^\perp(W), \quad \pi^\perp(W) = l(W) r_0 = \frac{\langle W, v_0 \rangle}{\langle r_0, v_0 \rangle} r_0$$

$$y = \pi(W) = W - \frac{\langle W, v_0 \rangle}{\langle r_0, v_0 \rangle} r_0.$$

The vectors r_0 and v_0 are evaluated for an averaged set of Jacobian matrices $\bar{A}$ and $\bar{B}$. From a physical point of view, $l(W)$ is the component of W on the entropy wave r_0, while $\pi(W)$ is the sum of the acoustic and shear waves.

The key remark is to notice that the N scheme and the LDA scheme have a simple expression for this decomposition because r_0 is a common eigenvector of $\bar{A}$ and $\bar{B}$. More precisely, we have

$$\Phi_i^N = \sum_{j=1; j \neq i}^{3} K_i^+ N K_j^- \pi^\perp (\tilde{W}_i - \tilde{W}_j) + \sum_{j=1; j \neq i}^{3} K_i^+ N K_j^- \pi (\tilde{W}_i - \tilde{W}_j)$$

$$= \left(\frac{\sum_{j=1; j \neq i}^{3} k_i^+ k_j^- l(W_i - W_j)}{\sum_{j=1,3} k_j^-} \right) r_0 + \sum_{j=1; j \neq i}^{3} K_i^+ N K_j^- \pi (\tilde{W}_i - \tilde{W}_j)$$

$$\Phi_i^{LDA} = - \sum_{j=1; j \neq i}^{3} K_i^+ N K_j \pi^\perp (\tilde{W}_i - \tilde{W}_j) - \sum_{j=1; j \neq i}^{3} K_i^+ N K_j \pi (\tilde{W}_i - \tilde{W}_j)$$

$$= \left(\frac{\sum_{j=1; j \neq i}^{3} k_i^+ k_j l(W_i - W_j)}{\sum_{j=1; j \neq i}^{3} k_i^+} \right) r_0 - \sum_{j=1; j \neq i}^{3} K_i^+ N K_j \pi (\tilde{W}_i - \tilde{W}_j).$$

For this reason, we set

$$\ell = l_1 \pi^\perp + l_2 \pi. \tag{40}$$

In other words, the matrix ℓ has two components. One acts only on the components on the entropy wave, and the other component only plays on the shear–acoustic waves. Then, thanks to Lemma 4.3, we evaluate the entropy production within a single triangle,

$$
\begin{aligned}
\langle v_i, \Phi_i \rangle &= \langle v_i, \ell\Phi_i^{\mathrm{N}} \rangle + \langle v_i, (Id - \ell)\Phi_i^{\mathrm{LDA}} \rangle \\
&= \left(l_1 \langle v_i, \pi^{\perp}(\Phi_i^{\mathrm{N}}) \rangle + (1 - l_1)\langle v_i, \pi^{\perp}(\Phi_i^{\mathrm{LDA}}) \rangle \right) \\
&\quad + \left(l_2 \langle v_i, \pi(\Phi_i^{\mathrm{N}}) \rangle + (1 - l_2)\langle v_i, \pi(\Phi_i^{\mathrm{LDA}}) \rangle \right) \\
&= \left(l_1 + (1 - l_1)\frac{\langle v_i, \pi^{\perp}(\Phi_i^{\mathrm{LDA}}) \rangle}{\langle v_i, \pi^{\perp}(\Phi_i^{\mathrm{N}}) \rangle} \right) \langle v_i, \pi^{\perp}(\Phi_i^{\mathrm{N}}) \rangle \\
&\quad + \left(l_2 + (1 - l_2)\frac{\langle v_i, \pi(\Phi_i^{\mathrm{LDA}}) \rangle}{\langle v_i, \pi(\Phi_i^{\mathrm{N}}) \rangle} \right) \langle v_i, \pi(\Phi_i^{\mathrm{N}}) \rangle .
\end{aligned}
$$

We define l_1 and l_2 by the two conditions

- For $i = 1, 2, 3,$

$$
l_1 + (1 - l_1)\frac{\langle v_i, \pi^{\perp}(\Phi_i^{\mathrm{LDA}}) \rangle}{\langle v_i, \pi^{\perp}(\Phi_i^{\mathrm{N}}) \rangle} \geq 0,
$$

- For $i = 1, 2, 3,$

$$
l_2 + (1 - l_2)\frac{\langle v_i, \pi(\Phi_i^{\mathrm{LDA}}) \rangle}{\langle v_i, \pi(\Phi_i^{\mathrm{N}}) \rangle} \geq 0.
$$

Following the developments of Section 5, we set

$$
\begin{aligned}
l_1 &= \min(1, \max(\varphi_{\xi}(r_1'), \varphi_{\xi}(r_2'), \varphi_{\xi}(r_3'))) \\
l_2 &= \min(1, \max(\varphi_{\xi}(r_1), \varphi_{\xi}(r_2), \varphi_{\xi}(r_3))),
\end{aligned}
\tag{41}
$$

where $r_i = \langle v_i, \pi(\Phi_i^{\mathrm{LDA}}) \rangle / \langle v_i, \pi(\Phi_i^{\mathrm{N}}) \rangle$ and $r_i' = \langle v_i, \pi^{\perp}(\Phi_i^{\mathrm{LDA}}) \rangle / \langle v_i, \pi^{\perp}(\Phi_i^{\mathrm{N}}) \rangle$ for $i = 1, 2, 3$, $\xi \in [0, 1[$, and φ_{ξ} is defined by (31). Contrary to the scalar case where the value of ξ, was unimportant, it is not clear whether different values of ξ furnish the same value of l_2. Another solution is given by

$$
\begin{aligned}
l_1 &= \min(1, \max(\psi(r_1'), \psi(r_2'), \psi(r_3'))) \\
l_2 &= \min(1, \max(\psi(r_1), \psi(r_2), \psi(r_3))),
\end{aligned}
\tag{42}
$$

where ψ is defined by (33).

Remark 6.1.

1. In the continuous case, we have $ds = \langle v, dW \rangle$. Since v belongs to $\mathbb{R}r_0$, v is orthogonal to the acoustic and shear modes of the Euler equations. In the discrete case, however, the situation is a bit more complex: There is no reason why $\langle v_i, \pi^{\perp}\Phi_i^{\mathrm{N}} \rangle$ should be zero. When the flow is smooth, $\langle v_i, \pi^{\perp}\Phi_i^{\mathrm{N}} \rangle$ is likely to be small, but certainly not when a discontinuity exists.

2. We have developed another version of the scheme (referred to as the V-scheme later in this remark), where we replace v by $V = \nabla_W(\rho s)$. At the continuous level, one has $\langle V, \operatorname{div} \mathbf{F}(W)\rangle = \rho \langle v, \operatorname{div} \mathbf{F}(W)\rangle + s \operatorname{div}(\rho \mathbf{u})$, and then

$$\langle V, \pi(\operatorname{div} \mathbf{F}(W))\rangle = \rho \langle v, \operatorname{div} \mathbf{F}(W)\rangle$$

and

$$\langle V, \pi^{\perp}(\operatorname{div} \mathbf{F}(W))\rangle = s \operatorname{div}(\rho \mathbf{u}).$$

This suggests that the same numerical technique, where v_i is replaced by V_i, would be a very similar scheme on $\mathbb{R}r_0$, but would act to limit the mass flow on H. We have implemented this scheme. Its results are indistinguishable from those obtained by the scheme (v-scheme) developed in this section. However, we have preferred the v-scheme because the interpretation of the V-scheme is not clear. The v-scheme uses an approximation of the transport of the physical entropy where a minimum principle exists, while the V-scheme uses an approximation of a conservation operator,

$$\frac{\partial(\rho s)}{\partial t} + \operatorname{div}(\rho s \mathbf{u})$$

for which no minimum or maximum principle exists.

7. BOUNDARY CONDITIONS

To set the boundary conditions, we utilize the fact that a finite volume scheme is a residual distributive scheme, according to Eq. (9). The inflow and outflow boundary conditions are prescribed via the modified Steger and Warming [8] flux splitting,

$$\mathcal{F}(W_i, W_\infty, \mathbf{n}) = A(W_i)^+ \cdot \mathbf{n} W_i + A(W_i)^- \cdot \mathbf{n} W_\infty,$$

and the wall conditions are simply obtained by setting $\langle \mathbf{u}, \mathbf{n} \rangle = 0$; i.e.,

$$\mathcal{F}_{\text{wall}}(W_i, \mathbf{n}) = \begin{pmatrix} 0 \\ pn_x \\ pn_y \\ 0 \end{pmatrix}.$$

8. NUMERICAL EXAMPLES

We have run this scheme on many examples; all of them are steady computations. We report the most significant ones and compare them with the N scheme, the LDA scheme, a first-order finite volume scheme (Roe scheme), and a monotonic upstream-centered scheme for conservation laws (MUSCL) (Roe scheme with MUSCL extrapolation on the primitive variables with van Leer limiter). The finite volume schemes use the dual-cell control volume formulation [8]. For a given problem and variable, the same isolines have been used to draw the pictures whatever the scheme. In all the numerical computations, we have taken the matrix ℓ defined by (42).
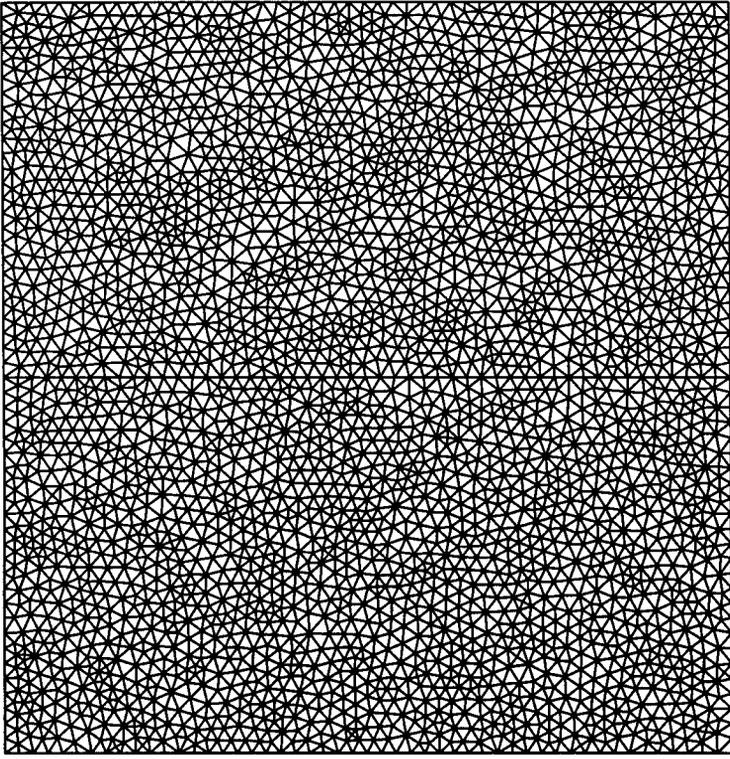
FIG. 3. Mesh for the shock tube problem.

8.1. *A Shock Tube Problem*

The initial condition consists of two parallel uniform flows, conditions of which are listed above:

- Top: Mach number $= 2.4$, $\rho = \gamma$, $p = 1$
- Bottom: Mach number $= 4$, $\rho = \frac{\gamma}{2}$, $p = 0.25$

The conditions on the left boundary are identical to the initial conditions. The flow is everywhere supersonic; no exit boundary condition is needed. The steady solution consists of a shock wave, a contact discontinuity, and a fan. On any line orthogonal to the initial velocity vector, the solution looks like a 1D Riemann problem. On Fig. 3, we display the mesh, on Figs. 4–6, the density, the pressure, and the Mach number.

From these results, it appears clearly that:

- the resolution of the shock between the MUSCL and blended schemes favors the new scheme,
- the resolution of the slip line between the MUSCL and blended schemes without any doubt favors the blended scheme,
- the fan is better represented by the blended scheme because the plateau, where the solution is constant between the discontinuities, starts earlier for the blended scheme than for MUSCL scheme.

The display of the results for the N scheme illustrates the monotonic behavior of this scheme, where as the LDA scheme is clearly not monotonic.
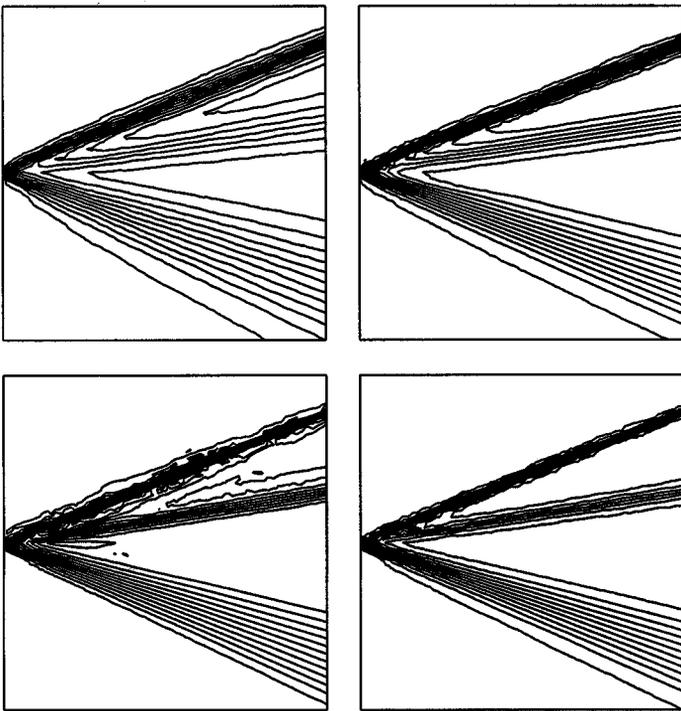
FIG. 4. Density isolines for the shock tube problem. Top: N scheme (left), MUSCL scheme (right). Bottom: LDA scheme (left), Blended scheme (right). N scheme: $0.7 \leq \rho \leq 1.4$, MUSCL: $0.69 \leq \rho \leq 1.40$, LDA: $0.61 \leq \rho \leq 1.42$, Blended: $0.70 \leq \rho \leq 1.40$.
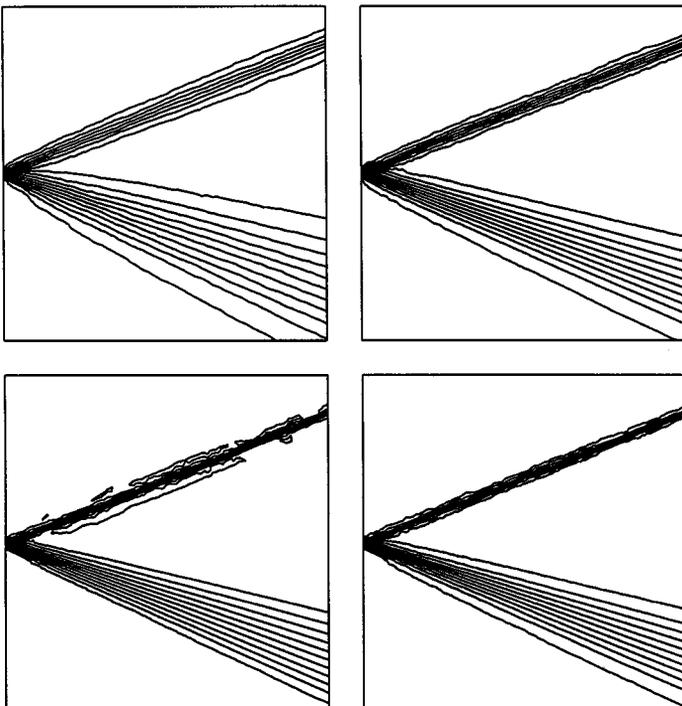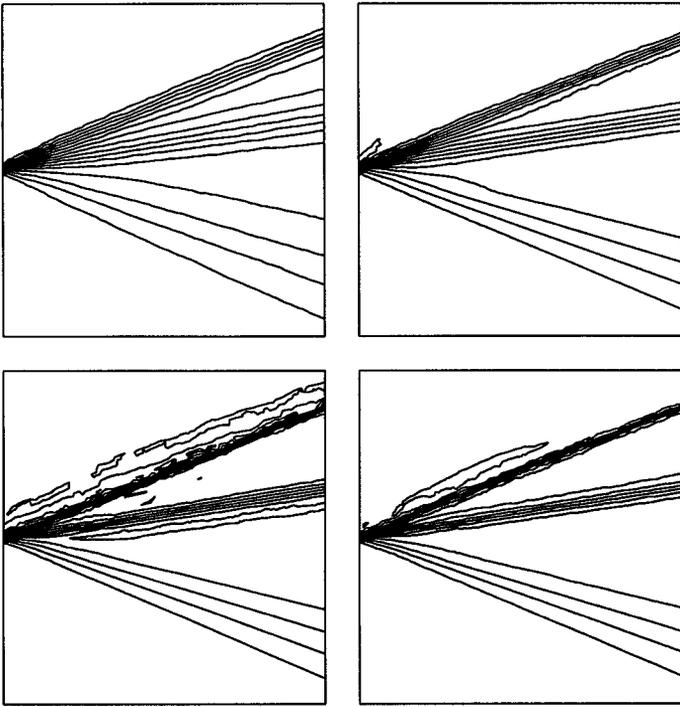

FIG. 5. Pressure isolines for the shock tube problem. Top: N scheme (left), MUSCL scheme (right). Bottom: LDA scheme (left), Blended scheme (right). N scheme: $0.25 \leq p \leq 1$, MUSCL: $0.24 \leq p \leq 1$, LDA: $0.2 \leq p \leq 1.04$, Blended: $0.25 \leq p \leq 1$.

FIG. 6. Mach number isolines for the shock tube problem. Top: N scheme (left), MUSCL scheme (right). Bottom: LDA scheme (left), Blended scheme (right). N scheme: $2.4 \leq M \leq 4$, MUSCL: $2.40 \leq M \leq 4.07$, LDA: $2.39 \leq M \leq 4.27$, Blended: $2.4 \leq M \leq 4.0$.

8.2. A Transonic Test Case

We take one of the test cases of the Game workshop held at INRIA Rocquencourt in 1987 [7]. It is the NACA 0012 case, the Mach number at infinity is $M_\infty = 0.85$, with $\alpha = 1°$. The solution has two shocks: one on the top of the airfoil, and a weaker one on its

(a)   (b)
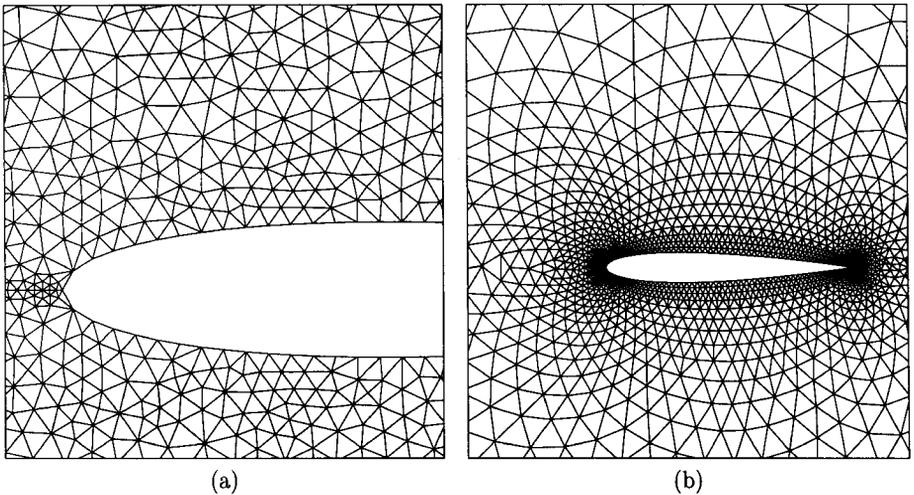
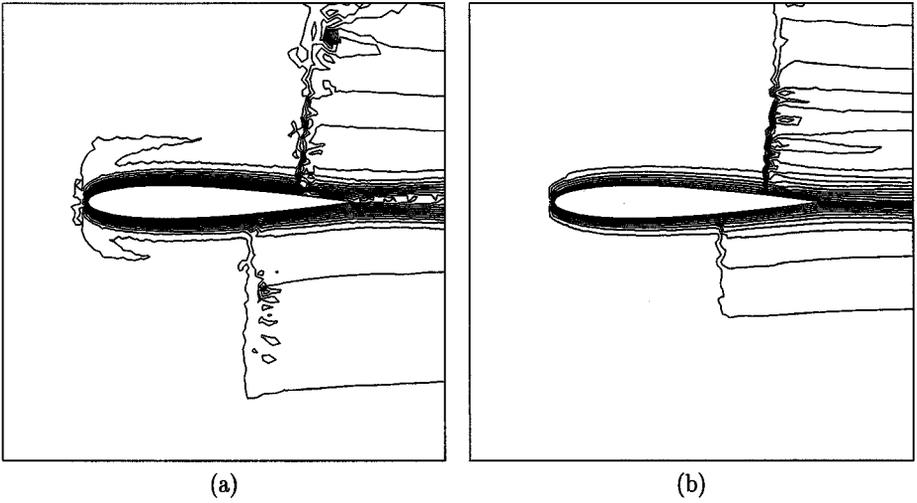**FIG. 7.** Meshes for the NACA 0012 problem.

FIG. 8. Deviation of physical entropy ($\Sigma = s - s_\infty/s_\infty$) for the MUSCL scheme (a) and the blended scheme (b).

bottom. A slip line comes out of the trailing edge. This case is interesting because the more dissipative the scheme, the more symmetric the solution. We present the results on two different meshes. Both are unstructured; one is very irregular (Fig. 7a); the other is much more regular (Fig. 7b). Our purpose is to illustrate the effects of the numerical dissipation and the mesh. Table I gives the minimum and maximum of the Mach number, the pressure coefficient $c_p = (p - p_\infty)/(\frac{1}{2}\rho_\infty u_\infty^2)$, and the entropy deviation $\Sigma = (s - s_\infty)/s_\infty$ for the irregular mesh (Figs. 8–10) and the Mach number for the regular one (Fig. 11). There are three main facts.

1. By looking at Table I and Fig. 8, we see that the entropy has a more physical behavior for the blended scheme than for the MUSCL scheme. There is no numerical artifact (see Fig. 8a, lower and upper shocks). The slip line seems less diffused. We should have $\Sigma \geq 0$.
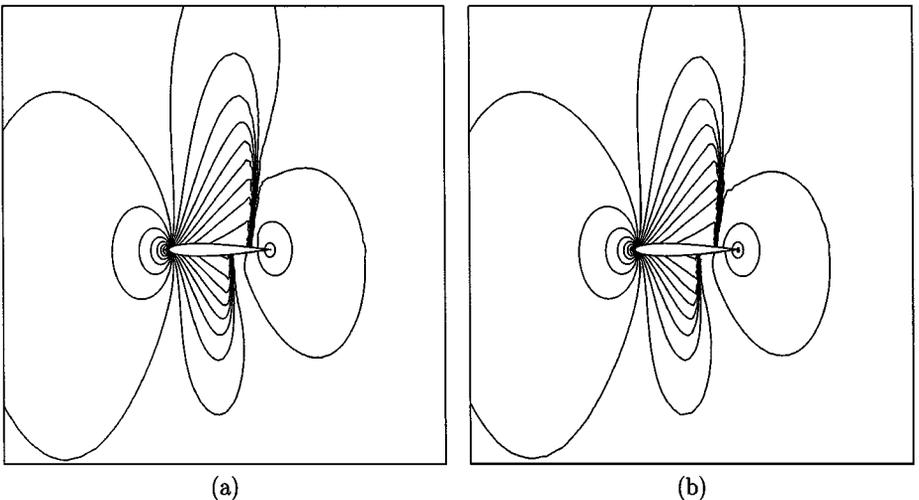

FIG. 9. Pressure coefficient for the MUSCL scheme (a) and the blended scheme (b).
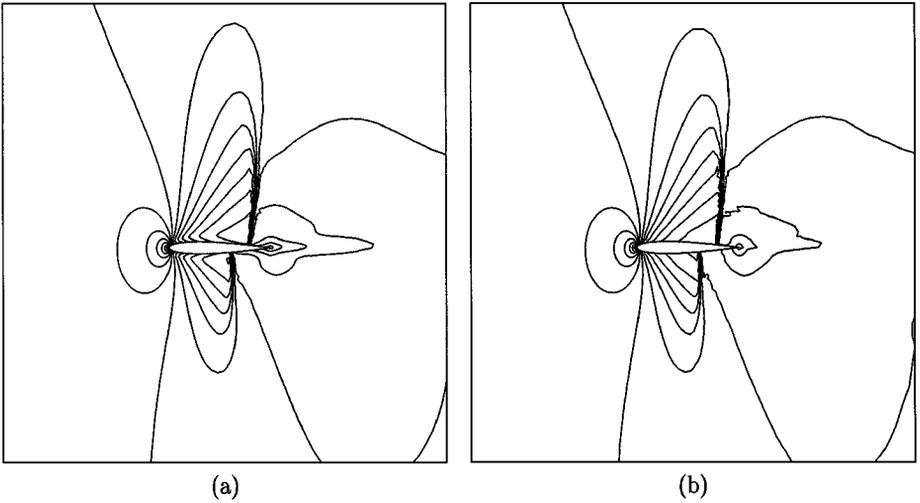
FIG. 10. Mach number contours for the MUSCL scheme (a) and the blended scheme (b).

Numerically this is violated by both schemes but by an order of magnitude less by the blended scheme; see Table I.

2. The shocks are better resolved because the isolines go into the shock much more for the blended scheme than for the MUSCL one; see Figs. 9 and 10.

3. When comparing the results of Fig. 10, one can see a strange behavior of the Mach number contours. This is due to the large entropy layer created by the MUSCL scheme and the strong dependency of the scheme on the mesh. Compare to Fig. 11, where the same schemes have been used on a much more regular mesh. There is still a larger entropy layer for the MUSCL scheme, but its influence on the Mach number is much weaker.
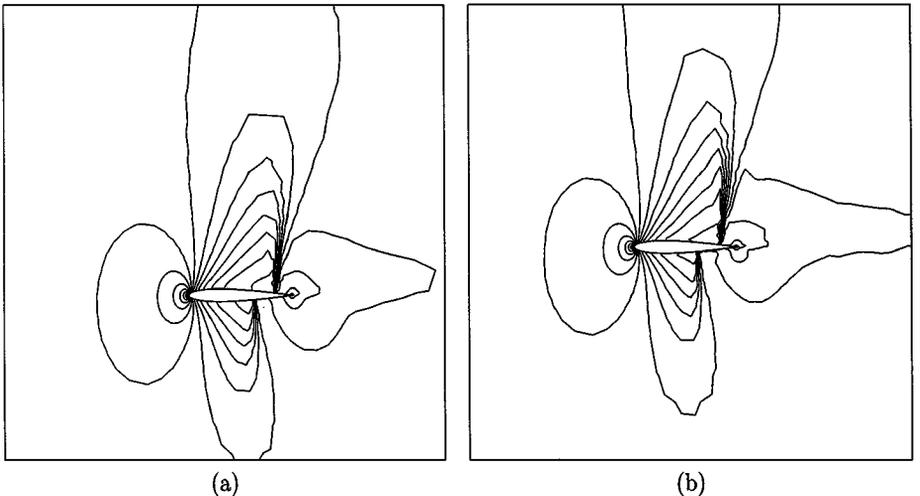

FIG. 11. Mach number contours on the regular mesh of Fig. 7b for the MUSCL scheme (a) and the blended scheme (b).

TABLE I
NACA 0012 Problem on 7a and b

Irregular Mesh, Figure 7a			
Scheme	Mach (Min, Max)	c_p (Min, Max)	Σ (Min, Max)
MUSCL	0.053, 1.34	−1.00, 1.05	−0.005, 0.054
Blended	0.022, 1.39	−1.00, 1.08	−0.0005, 0.052
Regular Mesh, Figure 7b			
Scheme		Mach (Min, Max)	
MUSCL		0.047, 1.42	
Blended		0.05, 1.43	

Note. Minimum and maximum of the Mach number, the pressure coefficient, and the entropy deviation.

8.3. *Engine Inlet*

This is another test case of the Gamm workshop [7]. The conditions are set so that the Mach number at infinity is $M_\infty = 2$ and the Mach number at the exit of the engine inlet is $M = 0.27$. We display in Fig. 12 the Mach number in the whole computational domain. The solution has a lambda shock at the entrance of the inlet. This lambda shock produces a slip line coming out of the triple point. By comparing the solutions of Figs. 12c and 12d, it is clear that a slip line is much better resolved by the blended scheme than the MUSCL one, even though the mesh is quite coarse; see Fig. 13.

Next, in Figs. 14–16, we see that the location of the secondary shock depends on the scheme. The shock is hardly visible for Roe's. By increasing strength, we have the N scheme first, then MUSCL, and last the blended scheme. Moreover, the stronger the scheme the further the shock is from the inlet entrance. This is quite consistent with the conclusion of the Gamm workshop: The less diffusive the shock is, the further from the entrance it is. We have run this case with the LDA scheme; the results are very oscillatory but support this conclusion. In Table II, one can notice that even if $\Sigma \geq 0$ theoretically, this is not the case for the new scheme. However, the deviation form $\Sigma \geq 0$ is more than an order of magnitude smaller from the blended than the MUSCL scheme.

Last, the lambda shock is reflected on the wall of the engine. The reflection is much clearer for the blended scheme than for the MUSCL one. The shock wave also has more reflections, but this is difficult to notice on Fig. 12.

TABLE II
Engine Inlet Problem

Scheme	Mach (Min, Max)	Pressure (Min, Max)	Σ (Min, Max)
Roe	0.50, 2.21	0.57, 5.76	0.0, 0.14
N	0.53, 2.25	0.58, 6.06	0.0, 0.10
MUSCL	0.48, 2.26	0.56, 5.90	−0.01, 0.16
Blended	0.38, 2.27	0.56, 6.75	−0.0008, 0.17

Note. Minimum and maximum of the Mach number, pressure, and entropy deviation Σ for the first-order Roe scheme, the N scheme, the MUSCL scheme, and the blended scheme.

(a)   (b)

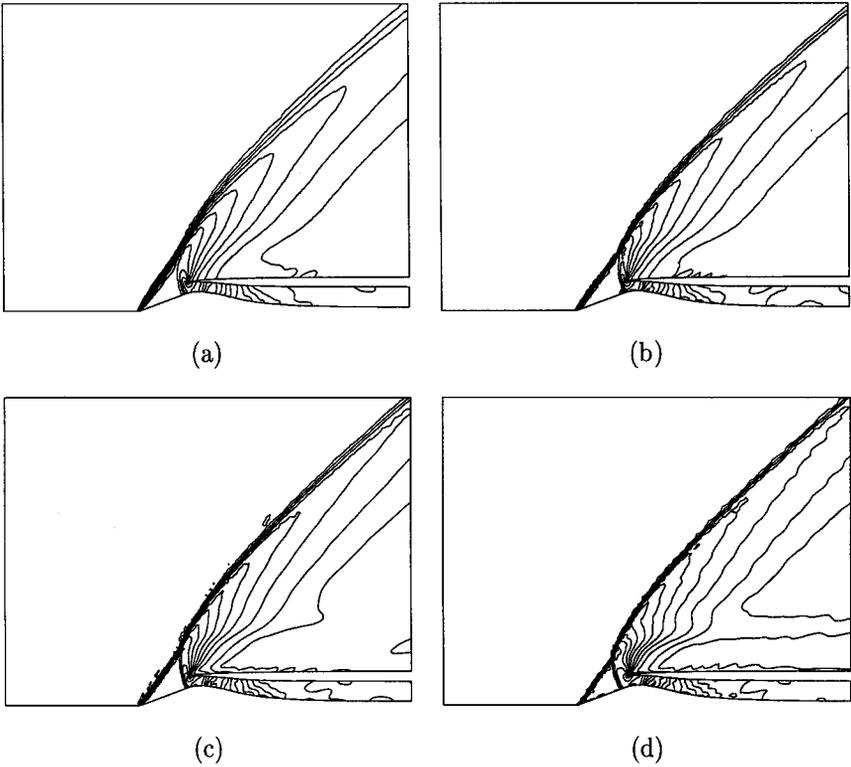(c)   (d)

FIG. 12. Mach number contours for the first-order Roe scheme (a), the system N scheme (b), the MUSCL scheme (c), and the blended scheme (d).

8.4. *Flow over a Cylinder*

This is another Gamm test case. The Mach number at infinity is $M_\infty = 0.38$. The solution should be symmetric with respect to the x and y axes. The Mach number is always less than 1, but its maximum is very close to 1. Since the flow is subsonic, the entropy deviation
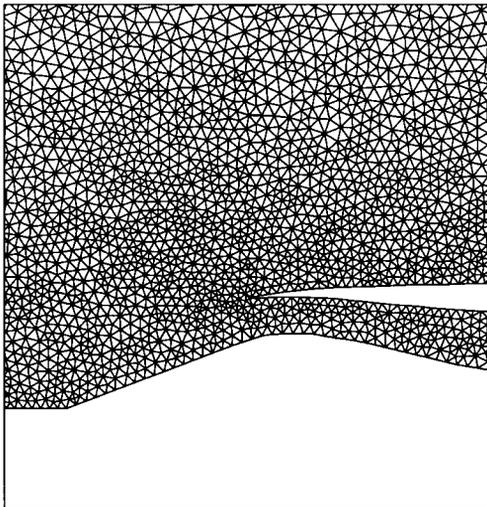

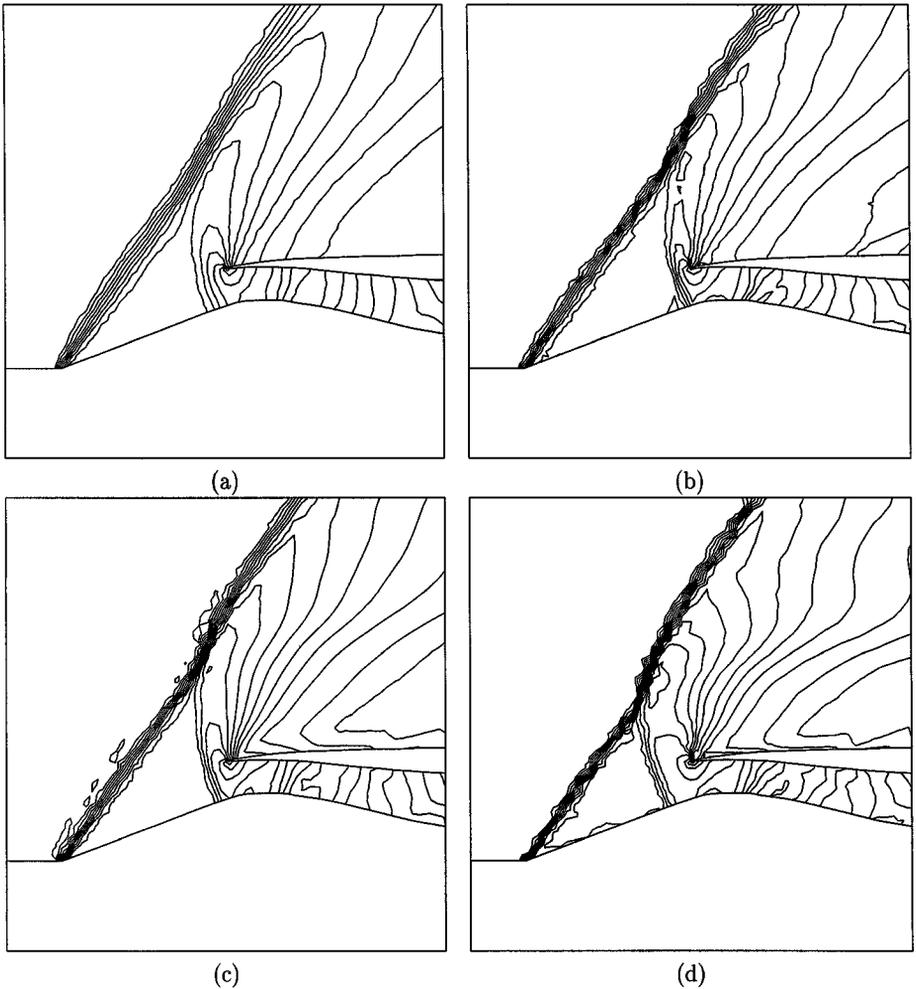**FIG. 13.** Zoom of the mesh near the inlet entrance.

FIG. 14. Zoom of the Mach number contours for the first-order Roe scheme (a), the system N scheme (b), the MUSCL scheme (c), and the blended scheme (d).

should be 0. In fact, the respect of the symmetry properties and the departure from $\Sigma = 0$ are good criteria to compare the solutions. Once more the mesh is completely unstructured; see Fig. 17.

We display the solution given by the MUSL scheme, the blended scheme, and the LDA scheme, As expected, the LDA scheme gives the best results; see Figs. 18c and 19c. But the blended scheme is not that far away; see Figs. 18b and 19b, and compare the max/min values on Table III. It also gives much better results than the MUSCL scheme, as reported on Figs. 18a and 19a, and Table III. The entropy production is five times greater than in the other schemes. The entropy layer is also much thicker.

8.5. *Comments on the Iterative Convergence*

As in the van der Weide system PSI scheme [15], the iterative convergence of the scheme we present in this paper is very poor; basically the L^2 residual on the density stagnates at about 10^{-2}–10^{-3}, where the residual is compared to the first iteration.
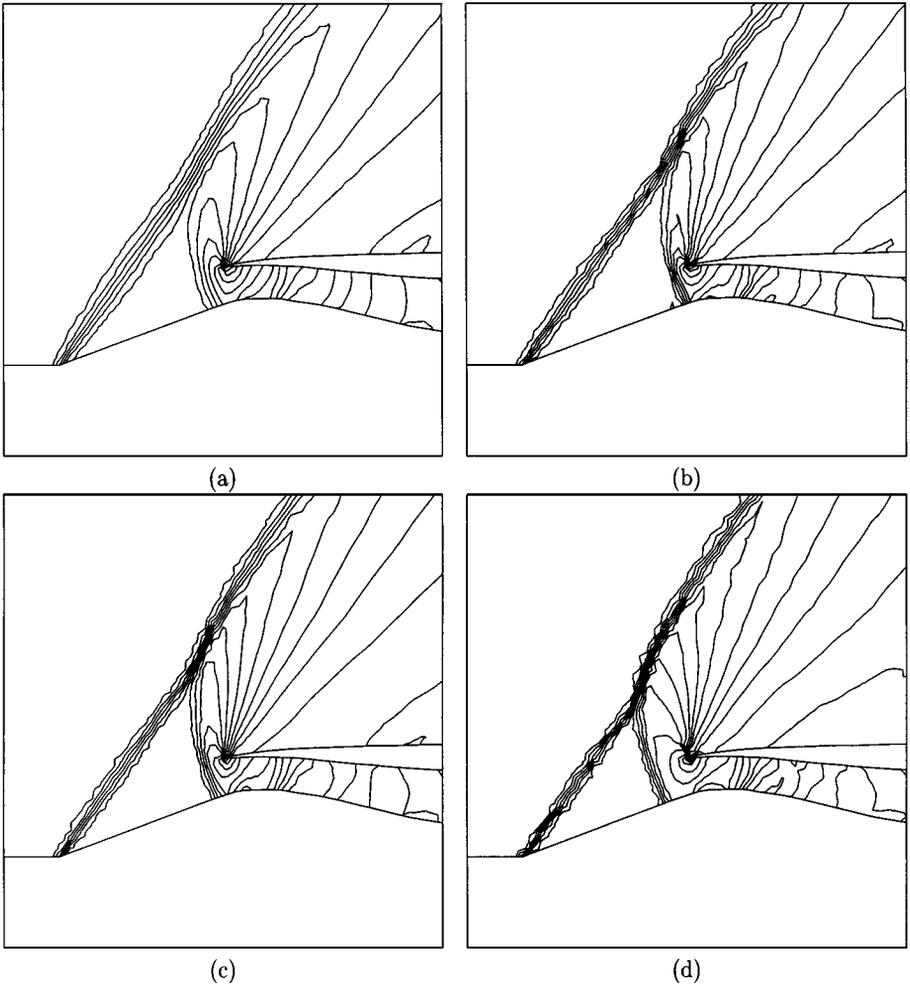
FIG. 15. Zoom of the pressure contours for the first-order Roe scheme (a), the system N scheme (b), the MUSCL scheme (c), and the blended scheme (d).

There is a way to improve this behavior by modifying the arguments in Eqs. (32) or (34). To simplify the text, take the example of the function ψ, Eqs. (33). The arguments are essentially

$$\psi(r_i) = \frac{\left|\langle v_i, \Phi_i^{\mathrm{LDA}} \rangle\right|}{\left|\langle v_i, \Phi_i^{\mathrm{LDA}} \rangle\right| + \left|\langle v_i, \Phi_i^{\mathrm{N}} \rangle\right|}$$

TABLE III
Flow over a Cylinder Problem

Scheme	Mach (Min, Max)	Pressure (Min, Max)	Σ (Min, Max)
MUSCL	0.0001, 0.82	0.67, 1.10	$-0.0004\ 0.048$
Blended	0.0001, 0.89	0.64, 1.11	0.0, 0.009
LDA	0.0, 0.94	0.62, 1.10	$-0.001, 0.010$

Note. Minimum and maximum of the mach number, pressure, and entropy deviation Σ for the MUSCL scheme, the blended scheme, and the LDA scheme.
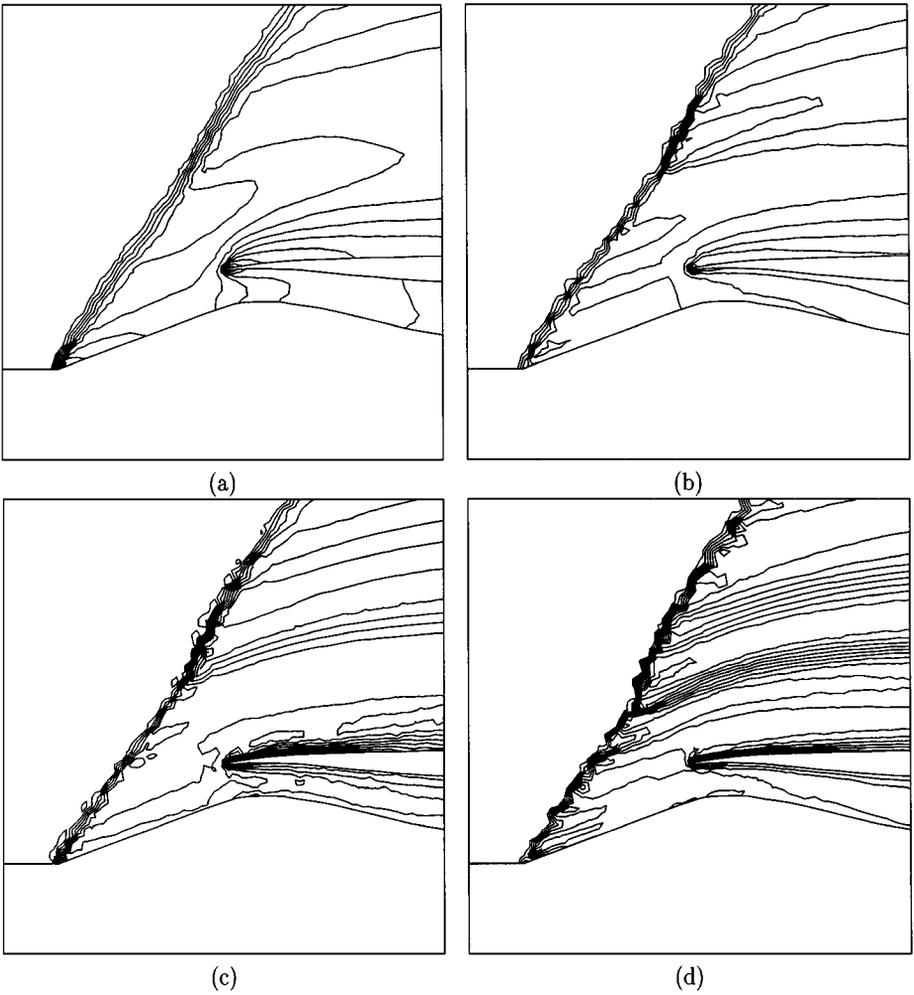
FIG. 16. Zoom of the entropy deviation contours for the first-order Roe scheme (a), the system N scheme (b), the MUSCL scheme (c), and the blended scheme (d).

or

$$\psi(r_i) = \frac{\left|\langle v_i, \pi^\perp \Phi_i^{\mathrm{LDA}}\rangle\right|}{\left|\langle v_i, \pi^\perp \Phi_i^{\mathrm{LDA}}\rangle\right| + \left|\langle v_i, \pi^\perp \Phi_i^{\mathrm{N}}\rangle\right|}.$$

To prevent division by zero, we have considered instead

$$\psi_\epsilon(r_i) = \frac{\left|\langle v_i, \Phi_i^{\mathrm{LDA}}\rangle\right|}{\left|\langle v_i, \Phi_i^{\mathrm{LDA}}\rangle\right| + \left|\langle v_i, \Phi_i^{\mathrm{N}}\rangle\right| + \epsilon}$$

and

$$\psi_\epsilon(r_i) = \frac{\left|\langle v_i, \pi^\perp \Phi_i^{\mathrm{LDA}}\rangle\right|}{\left|\langle v_i, \pi^\perp \Phi_i^{\mathrm{LDA}}\rangle\right| + \left|\langle v_i, \pi^\perp \Phi_i^{\mathrm{N}}\rangle\right| + \epsilon}.$$
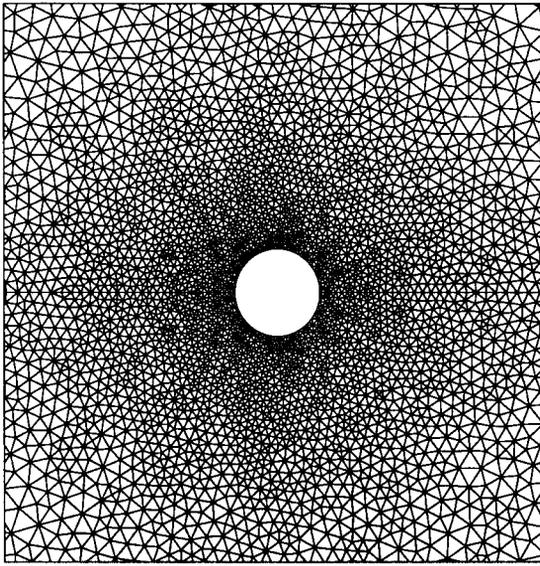
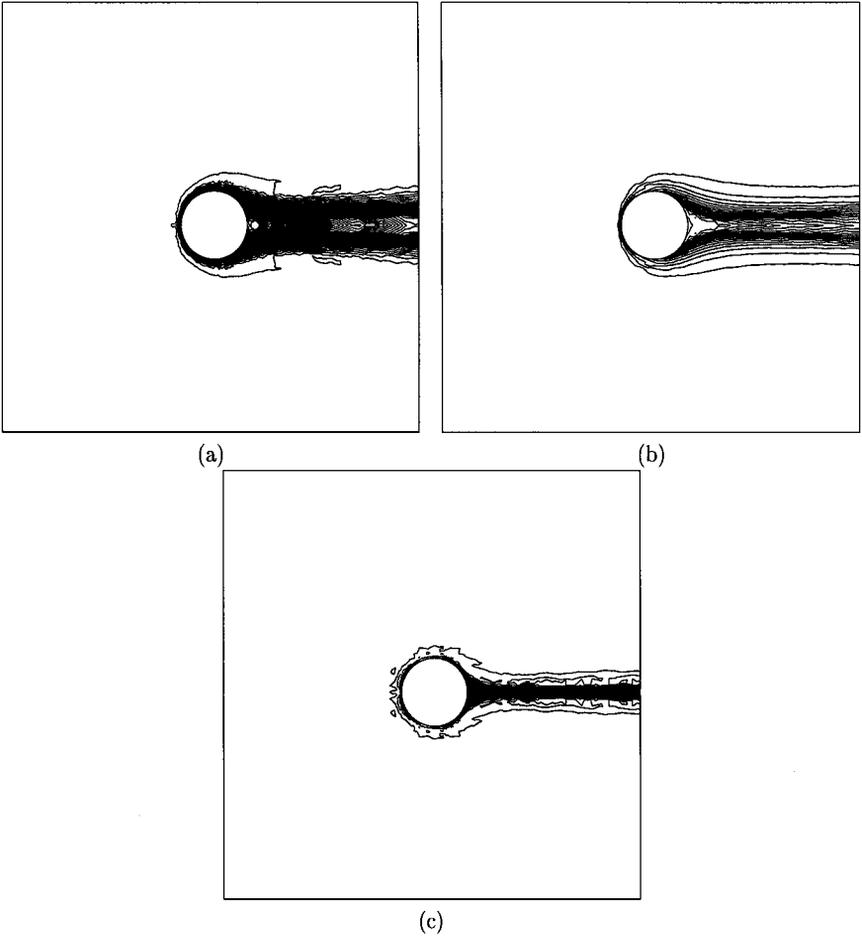**FIG. 17.** Mesh for the cylinder problem.

(a)

(b)

(c)

FIG. 18. Entropy deviation contours for the MUSCL scheme (a), the blended scheme (b), and the LDA scheme (c).
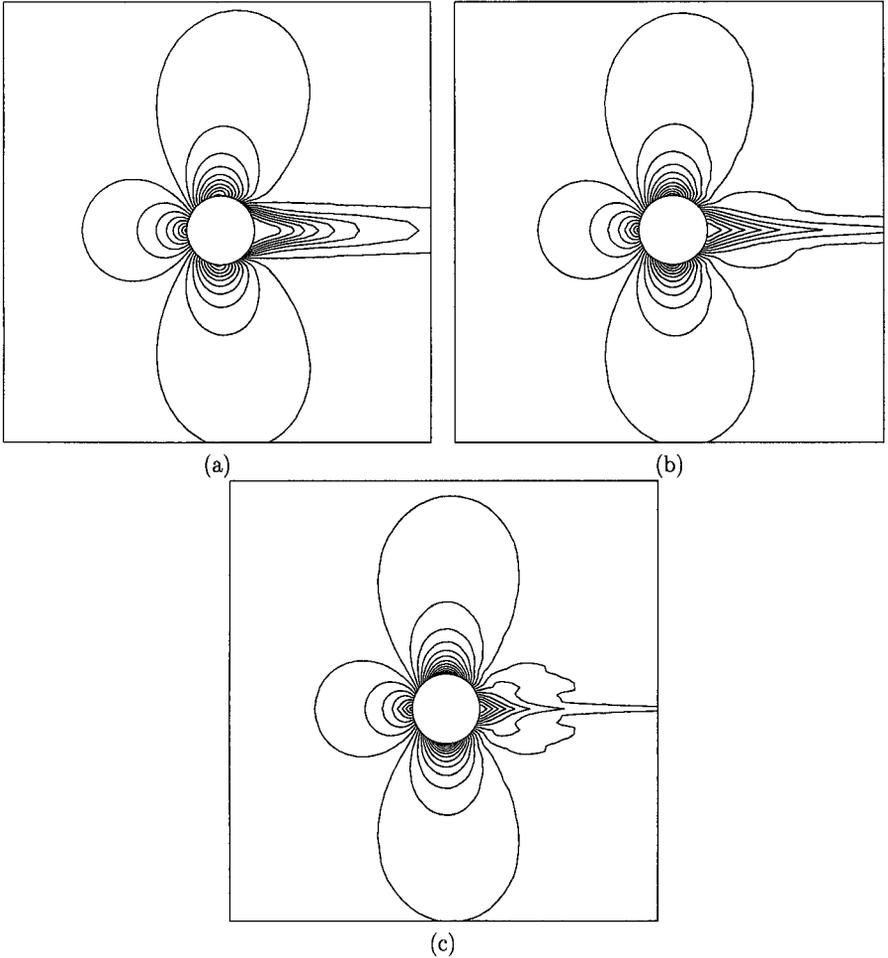
FIG. 19.   Mach number contours for the MUSCL scheme (a), the blended scheme (b), and the LDA scheme (c).

The parameter ϵ should be $O(h^3)$ for it to be negligible compared to the residual of the N and LDA schemes. In all the calculations, we have set ϵ in the range $[10^{-5}, 10^{-6}]$. If ϵ is too small, the iterative convergence is erratic. If $\epsilon \to 0$ the scheme resembles the LDA scheme. In our experiments, we have noticed that the results are quite insensitive to ϵ: they are nonoscillatory.

9. CONCLUDING REMARKS

In this paper, we have presented the construction of an upwind residual scheme that is formally second-order accurate at steady state. It is a blending between the system N scheme and the low diffusion advection schemes formally extended by van der Weide and Deconinck. The present construction relies on the analysis of the entropy production of the scheme within a single element. This scheme is robust and much less diffusive than a state-of-the-art MUSCL scheme on an unstructured mesh. The stencil of the scheme is also more compact, so a parallel implementation is much easier.

The limiter we consider here has only two degrees of freedom. Future work will consist of constructing limiters with more parameters, in the hope of decreasing the numerical diffusion. Extensions to unsteady flows will also be considered.

APPENDIX A

Proof of Lemma 4.1

The proof of the energy inequality was made by T. Barth and is presented in [2]. It is included in the present paper for completeness, with permission from the original author.

For ease of exposition, we will show the development in two space dimensions, but the generalization to $\mathbb{R}^d$ will be clear. The analysis is done for a symetrized linear hyperbolic system: we assume that the matrices K_i are symmetric, the state variables are V_i.

Setting $V = (V_1, V_2, V_3)^T$, we can rewrite the N scheme as

$$L_T V_T = \begin{pmatrix} \Phi_1 \\ \Phi_2 \\ \Phi_3 \end{pmatrix} = \left[\begin{bmatrix} K_1^+ & & \\ & K_2^+ & \\ & & K_3^+ \end{bmatrix} + \begin{bmatrix} K_1^+ \\ K_2^+ \\ K_3^+ \end{bmatrix} [N] \begin{bmatrix} K_1^- \\ K_2^- \\ K_3^- \end{bmatrix}^T \right] \begin{pmatrix} V_1 \\ V_2 \\ V_3 \end{pmatrix} \quad (43)$$

with $K^\pm$ symmetric and $[N]$ a block diagonal matrix $[N] \equiv \mathrm{diag}(N, N, N)$.

The study of the quadratic form

$$\langle V_1, \Phi_1 \rangle + \langle V_2, \Phi_2 \rangle + \langle V_3, \Phi_3 \rangle$$

amounts to studying the symmetric matrix $(L + L^T)/2$. The study of $\mathcal{Q}_N$,

$$\mathcal{Q}_N(V_1, V_2, V_3) = \langle V_1, \Phi_1 \rangle + \langle V_2, \Phi_2 \rangle + \langle V_3, \Phi_3 \rangle - \frac{1}{2} \left(\sum_{i=1}^{3} \langle V_i, K_i V_i \rangle \right),$$

is thus equivalent to the study of

$$\frac{1}{2}(L + L^T) - \frac{1}{2} \begin{bmatrix} K_1 & & \\ & K_2 & \\ & & K_3 \end{bmatrix}.$$

The symmetric part of L is given by

$$L_T = \begin{bmatrix} K_1^+ & & \\ & K_2^+ & \\ & & K_3^+ \end{bmatrix} + \frac{1}{2} \begin{bmatrix} K_1^+ \\ K_2^+ \\ K_3^+ \end{bmatrix} [N] \begin{bmatrix} K_1^- \\ K_2^- \\ K_3^- \end{bmatrix}^T + \frac{1}{2} \begin{bmatrix} K_1^- \\ K_2^- \\ K_3^- \end{bmatrix} [N] \begin{bmatrix} K_1^+ \\ K_2^+ \\ K_3^+ \end{bmatrix}^T . \quad (44)$$

Examining rows of L_T or L_T, observe that the row sum is nonzero. However, we can add the a block diagonal matrix to the element matrix L,

$$-\frac{1}{2} \begin{bmatrix} K_1 & & \\ & K_2 & \\ & & K_3 \end{bmatrix}, \quad (45)$$

so that rows and columns of the L_T sum to zero. These additional terms have no impact on the constant coefficient discretization of the Cauchy problem. These terms all vanish identically when summed for all elements sharing a mesh vertex since the geometry surrounding the vertex is closed. Henceforward, we will include these terms in our definition of L_T and T_T yielding

$$L_T = \frac{1}{2}\begin{bmatrix} |K|_1 & & \\ & |K|_2 & \\ & & |K|_3 \end{bmatrix} + \frac{1}{2}\begin{bmatrix} K_1^+ \\ K_2^+ \\ K_3^+ \end{bmatrix}[N]\begin{bmatrix} K_1^- \\ K_2^- \\ K_3^- \end{bmatrix}^T + \frac{1}{2}\begin{bmatrix} K_1^- \\ K_2^- \\ K_3^- \end{bmatrix}[N]\begin{bmatrix} K_1^+ \\ K_2^+ \\ K_3^+ \end{bmatrix}^T . \tag{46}$$

Next, rewrite off-diagonal terms such as

$$K_i^+ N K_j^- + K_i^- N K_j^+$$

in the following form:

$$K_i^+ N K_j^- + K_i^- N K_j^+ = K_i N K_j - K_i^+ N K_j^+ - K_i^- N K_j^- .$$

Consequently, L_T can be rewritten as

$$L_T = \frac{1}{2}\begin{bmatrix} K_1 \\ K_2 \\ K_3 \end{bmatrix}[N]\begin{bmatrix} K_1 \\ K_2 \\ K_3 \end{bmatrix}^T + \frac{1}{2}\begin{bmatrix} K_1^+ & & \\ & K_2^+ & \\ & & K_3^+ \end{bmatrix} - \begin{bmatrix} K_1^+ \\ K_2^+ \\ K_3^+ \end{bmatrix}[N]\begin{bmatrix} K_1^+ \\ K_2^+ \\ K_3^+ \end{bmatrix}^T$$

$$+ \frac{1}{2}\begin{bmatrix} -K_1^- & & \\ & -K_2^- & \\ & & -K_3^- \end{bmatrix} - \begin{bmatrix} -K_1^- \\ -K_2^- \\ -K_3^- \end{bmatrix}[N]\begin{bmatrix} -K_1^- \\ -K_2^- \\ -K_3^- \end{bmatrix}^T . \tag{47}$$

Note that the first term appearing on the right-hand side of Eq. (47) gives rise to a quadratic form with positive energy, so our only concern is the remaining terms on the right-hand side on this equation. Before proving positive semidefiniteness of (47), we first review a simple result concerning the spectra of noncommuting matrices.

LEMMA A.1.   *The nonzero parts of the spectrum of AB and BA are identical for all matrices $A \in \mathbb{R}^{m \times n}$ and $B \in \mathbb{R}^{n \times m}$.*

Proof.   See for example Axelsson [16, p. 69].   ■

Next we prove positive semidefiniteness of a specialized matrix in product form.

LEMMA A.2 (Golub).   *The matrix*

$$L = \begin{bmatrix} A & 0 & 0 \\ 0 & B & 0 \\ 0 & 0 & C \end{bmatrix} - \begin{bmatrix} A \\ B \\ C \end{bmatrix} N \begin{bmatrix} A \\ B \\ C \end{bmatrix}^T , \quad N = [A + B + C]^{-1},$$

is positive semidefinite for all $A, B, C \in \mathbb{R}^{n \times n}$ symmetric positive definite.

Proof. Let

$$Z = \begin{bmatrix} A & 0 & 0 \\ 0 & B & 0 \\ 0 & 0 & C \end{bmatrix}$$

and congruence transform L

$$Z^{-1/2} L Z^{-1/2} = \begin{bmatrix} I_n & & \\ & I_n & \\ & & I_n \end{bmatrix} - \begin{bmatrix} A^{1/2} \\ B^{1/2} \\ C^{1/2} \end{bmatrix} N \begin{bmatrix} A^{1/2} \\ B^{1/2} \\ C^{1/2} \end{bmatrix}^T = I_{3n} - P.$$

Next use Lemma A.1 concerning the spectra of nonsquare matrix products. In the present case Lemma A.1 implies that

$$\text{Eigenvalues}\left(\begin{bmatrix} A^{1/2} \\ B^{1/2} \\ C^{1/2} \end{bmatrix} N \begin{bmatrix} A^{1/2} \\ B^{1/2} \\ C^{1/2} \end{bmatrix}^T \right) = \text{Eigenvalues}\left(N^{1/2}(A + B + C)N^{1/2} \right) + 2n \text{ zeros}$$

$$= \text{Eigenvalues}(N(A + B + C)) + 2n \text{ zeros}$$
$$= \text{Eigenvalues}(I_n) + 2n \text{ zeros} \qquad (48)$$

and consequently

$$I_{3n} - P$$

is positive semidefinite. From this result it follows immediately that

$$L = Z^{1/2}(I_{3n} - P)Z^{1/2}$$

is also positive semidefinite.   ∎

The extension to $A, B, C \geq 0$ and $(A + B + C) > 0$ follows by considering the perturbed matrices $A_\epsilon = A + \epsilon I$, $B_\epsilon = B + \epsilon I$, and $C_\epsilon = C + \epsilon I$ and letting $\epsilon \downarrow 0$.

Returning to the system N scheme, we now can prove

LEMME A.3 (Lemma 4.1).   *If the matrices K_i are symmetric, one has*

$$\sum_{M_i \in T} \langle V_i, \Phi_i^T \rangle = \frac{1}{2} \sum_{M_i \in T} \langle V_i, K_i V_i \rangle + \mathcal{Q}_N(V_1, V_2, V_3), \qquad (49)$$

where

$$2\mathcal{Q}_N(V_1, V_2, V_3) = -\langle \Phi^T N, \Phi^T \rangle + \sum_{M_i \in T} (\langle V_i, K_i^+ V_i \rangle - \langle K_i^+ V_i, N K_i^+ V_i \rangle)$$

$$+ \sum_{M_i \in T} (\langle V_i, -K_i^- V_i \rangle - \langle -K_i^+ V_i, N(-K_i^-)V_i \rangle). \qquad (50)$$

The quadratic form $\mathcal{Q}_N$ is positive: the N scheme is locally dissipative.

Proof. Since $N = [K_1^+ + K_2^+ + K_3^+]^{-1} = [-K_1^- - K_2^- - K_3^-]^{-1}$, the result follows immediately after application of the Golub lemma to (47). ■

APPENDIX B

The N and LDA Schemes are Well Defined

We show that for a linearized symetrizable system, the system N and LDA schemes are well defined. We carry out the proof only for the N scheme; the extension to the LDA one is obvious.

We consider a linearization of the system

$$W_t + AW_x + BW_y = 0$$

by means of some parameter vector. The Jacobian is evaluated at some average state, for example, that given by the parameter vector Z. It could be any other linearization provided the symetrization property of the system is kept.

Formally, the residual within a triangle T of the system N scheme is written

$$\Phi_i^N = \sum_{M_j \in T} C_{ij}(\tilde{W}_i - \tilde{W}_j),$$

where the matrices C_{ij} are

$$C_{ij} = K_i^+ \left(\sum_{l=1,3} K_l^- \right)^{-1} K_j^-. \tag{51}$$

Here $K_l = An_x^l + Bn_y^l$, where (n_x^l, n_y^l) are the component of a vector $\mathbf{n}_l$. The vectors $\mathbf{n}_l$, $l = 1, 2, 3$ satisfy $\sum_{l=1}^3 \mathbf{n}_l = 0$. In the following, we set $N = (\sum_{l=1,3} K_l^-)^{-1}$. The question is whether the matrices C_{ij} are well defined.

Since the system is symmetrizable, there exists a symmetric positive definite (s.d.p.) matrix A_0 such that

$$\tilde{A} = AA_0^{-1}, \quad \tilde{B} = BA_0^{-1}$$

are symmetric. Here, A_0 is the Hessian of the mathematical entropy S evaluated at the average state. We set $\tilde{K}_l = \tilde{A}n_x^l + \tilde{B}n_y^l = K_l A_0^{-1}$. Since A_0 is s.d.p., we can left and right multiply by $A_0^{1/2}$ to see that

$$\tilde{K}_l^+ = K_l^+ A_0^{-1}, \quad \tilde{K}_l^- = K_l^- A_0^{-1}, \quad |\tilde{K}_l| = |K| A_0^{-1}.$$

We also have $\sum_l K_l = 0$, $\sum_l \tilde{K}_l = 0$.

Since $\tilde{A}$ and $\tilde{B}$ are symmetric, the $\tilde{K}_l$, $\tilde{K}_l^\pm$, $|\tilde{K}_l|$ are also symmetric. Hence

$$\sum_l \tilde{K}_l^+ \geq 0$$

$$\sum_l \tilde{K}_l^- \leq 0$$

$$\sum_l |\tilde{K}_l| \geq 0.$$

This shows that $\sum_l |K_l|$, $\sum_l K_l^+$, $-\sum_l K_l^-$ have positive eigenvalues; this can be seen still by left and right multiplying by $A_0^{1/2}$ and $A_0^{-1/2}$.

If one matrix K_l^+ has a system of strictly positive eigenvalues, $\sum_l K_l^+$ has only strictly positive eigenvalues. Thus $\sum_l K_l^+$ is invertible.

Assume now there exists $x \in \mathbb{R}^4$ such that $\sum_l K_l^+ x = 0$. By setting $y = A_0 x$, we have $\sum_l \tilde{K}_l^+ y = 0$. Thus,

$$0 = \left\langle \sum K_l^+ x, x \right\rangle = \sum_l \langle \tilde{K}_l^+ y, y \rangle.$$

If there exists l such that $\langle \tilde{K}_l^+ y, y \rangle > 0$, y cannot be in the kernel of $\sum \tilde{K}_i^{'+}$ unless $y = 0$ and then $x = 0$.

Thus we have to assume that $\tilde{K}_l^+ y = 0$ for $l = 1, 2, 3$. Since $\sum \tilde{K}_l^+ = -\sum \tilde{K}_l^-$, the same arguments as above, applied to $\tilde{K}_l^-$, show that $\tilde{K}_l^- y = 0$ for $l = 1, 2, 3$. Thus $K_l x = 0$, with $x \neq 0$. Coming back to the definition of K_l, since any two among $\{\mathbf{n}_1, \mathbf{n}_2, \mathbf{n}_3\}$ are linearly independent, we have $Ax = Bx = 0$: The matrices A and B have a common eigenvector, associated to the eigenvalue 0.

In the case of the Euler equations, the eigenvectors of A are

$$R_1^+ = \begin{pmatrix} 1 \\ u+a \\ v \\ H+ua \end{pmatrix}, \quad R_1^- = \begin{pmatrix} 1 \\ u-a \\ v \\ H-ua \end{pmatrix}, \quad R_1^0 = \begin{pmatrix} 1 \\ u \\ v \\ \frac{u^2+v^2}{2} \end{pmatrix}, \quad R_1^t = \begin{pmatrix} 0 \\ 0 \\ 1 \\ v \end{pmatrix}$$

with the eigenvalues $u+a$, $u-a$, u, and u. Those of B are

$$R_2^+ = \begin{pmatrix} 1 \\ u \\ v+a \\ H+ua \end{pmatrix}, \quad R_2^- = \begin{pmatrix} 1 \\ u \\ v-a \\ H-ua \end{pmatrix}, \quad R_2^0 = \begin{pmatrix} 1 \\ u \\ v \\ \frac{u^2+v^2}{2} \end{pmatrix}, \quad R_2^t = \begin{pmatrix} 0 \\ -1 \\ 0 \\ u \end{pmatrix}$$

with the eigenvalues $v+a$, $v-a$, v, and v. We see that $R_1^0 = R_2^0 = r_0$.

The only solution to the problem is $u = v = 0$ and $x = \lambda r_0 = \lambda r_0$ (stagnation point); otherwise $a = 0$, which corresponds to vacuum.

What remains is to show that one can give a meaning to C_{il} even in that case. More precisely, we show there exists a decomposition of $\mathbb{R}^4$ such that $\mathbb{R}^4 = \mathbb{R} r_0 \oplus H$, where H contains all the eigenvectors of A and B that are different from r_0.

LEMMA B.1. *If A and B are two matrices with one common eigenvector r_0, and if there exists a s.p.d. matrix A_0 that symmetrizes A and B there exists a vector space H that can be explicitly computed such that the other eigenvectors of A and B belong to H and $\mathbb{R}^n = (\mathbb{R} r_0) \oplus H$.*

Proof. The matrices AA_0^{-1} and BA_0^{-1} are symmetric; so are $A_0^{1/2} AA_0^{-1/2}$ and $A_0^{1/2} BA_0^{-1/2}$ (left and right multiply by $A_0^{1/2}$). They are also congruent to A and B, respectively.

Let $\{r_k\}_{k=0,n-1}$ and $\{r_k'\}_{k=0,n-1}$ complete systems of eigenvectors of A and B, respectively. We assume $r_0 = r_0'$. Then $\{A_0^{1/2} r_k\}_{k=0,n-1}$ and $\{A_0^{1/2} r_k'\}_{k=0,n-1}$ are complete systems of eigenvectors of symmetric matrices: They are orthogonal. Hence

$$\mathbb{R}^n = \mathbb{R} A_0^{1/2} r_0 \oplus \left(\mathbb{R} A_0^{1/2} r_0\right)^\perp.$$

Clearly , $A_0^{1/2} r'_k \in (\mathbb{R} A_0^{1/2} r_0)^\perp$ and $A_0^{1/2} r_k \in (\mathbb{R} A_0^{1/2} r_0)^\perp$ for $k > 0$. By defining

$$H = A_0^{-1/2} (\mathbb{R} A_0^{1/2} r_0)^\perp$$

we have the expected decomposition ■

$$x = l(x) r_0 + x^\perp, \quad x^\perp \in H,$$

where $l(x) = \frac{\langle A_0 x, x \rangle}{\langle A_0 r_0, r_0 \rangle}$, and we have

$$M_{ij} x = \left(\frac{\langle \mathbf{u}, \mathbf{n}_i \rangle^+ \langle \mathbf{u}, \mathbf{n}_j \rangle^-}{\sum_{i=1,3} \langle \mathbf{u}, \mathbf{n}_i \rangle^+} \right) l(x) r_0 + M_{ij} x^\perp.$$

When $\mathbf{u} \to 0$, the first term tends to 0 because

$$\left| \frac{\langle \mathbf{u}, \mathbf{n}_i \rangle^+ \langle \mathbf{u}, \mathbf{n}_j \rangle^-}{\sum_{i=1,3} \langle \mathbf{u}, \mathbf{n}_i \rangle^+} \right| \leq |\langle \mathbf{u}, \mathbf{n}_j \rangle^-| \to 0$$

and $M_{ij} x^\perp$ converges to a finite limit because none of the eigenvalues of the restriction of N to the space H vanish. ■

Remark B.2. Since $\pi^* A_0 = A_0 \pi$, we can see that $A_0 r_0 = v_0$. Hence H is the kernel of $\pi^\perp$.

APPENDIX C

Proof of Lemmas 4.2 and 4.3

In this section, we assume that the linearization is done via the entropy variable V and we use the notation of the previous section.

Throughout this section, we can assume the N, at least for the symmetrizable system, of the Euler equations. We set $M = -N$ and

$$V^+ = M \left(\sum_{i=1,3} \tilde{K}_i^+ V_i \right)$$

$$V^- = N \left(\sum_{i=1,3} \tilde{K}_i^- V_i \right),$$

so that we have $\Phi^T = M^{-1} (V^+ - V^-)$.

Proof of Lemma 4.2. A direct calculation shows (with obvious notation)

$$\mathcal{Q}_{\text{LDA}}(V_1, V_2, V_3) - \mathcal{Q}_{\text{N}}(V_1, V_2, V_3) = \sum_{i=1}^{3} \left\langle V_i, \Phi_i^{\text{LDA}} - \Phi_i^{\text{N}} \right\rangle.$$

Since $\Phi_i^{\text{LDA}} - \Phi_i^{\text{N}} = \tilde{K}_i^+(V^+ - V_i)$ and since

$$\sum_{i=1}^{3} K_i^+ V^+ = \sum_{i=1}^{3} K_i^+ V_i,$$

we get

$$\mathcal{Q}_{\text{LDA}}(V_1, V_2, V_3) - \mathcal{Q}_{\text{N}}(V_1, V_2, V_3) = \sum_{i=1}^{3} \langle V_i, \tilde{K}_i^+(V^- - V_i)\rangle$$

$$= -\sum_{i=1}^{3} \langle V^- - V_i, \tilde{K}_i^+(V^- - V_i)\rangle$$

$$\leq 0. \qquad \blacksquare$$

Proof of Lemma 4.3. The result is true if the first part of the lemma is shown. The N scheme can be written (in symmetric variables)

$$\Phi_i = \sum_{j=1}^{3} \tilde{K}_i^+ \tilde{N} \tilde{K}_j^- (V_i - V_j).$$

Since $\tilde{K}_i^+ = K_i^+ A_0^{-1}$, $\tilde{K}_j^- = K_j^- A_0^{-1}$, and $\tilde{N} = A_0 N$, we have

$$\Phi_i = \sum_{j=1}^{3} K_i^+ N K_j^- A_0^{-1} (V_i - V_j).$$

Now, π commutes with K_i^+, K_j^-, and N, and since $\pi^2 = \pi$ and $\pi A_0 = A_0 \pi^*$, we get the result for the N scheme. The proof is identical for the LDA scheme. The second part of the lemma is a consequence of its first part.

APPENDIX D

The Blended Scheme is LP at Convergence

To show that the blended scheme is LP at convergence, we have to check the condition (15) when the arguments in the residuals are replaced by the exact smooth solution. Here,

$$\sum_{T} \sum_{M_i \in T} \left(\varphi_i - \varphi_G^T\right) \cdot \Phi_i^T = \sum_{T} \sum_{M_i \in T} \left(\varphi_i - \varphi_G^T\right) \cdot \left(\Phi_i^{\text{LDA}} + \ell\left(\Phi_i^{\text{N}} - \Phi_i^{\text{LDA}}\right)\right).$$

The LDA scheme is LP because the matrices $-K_i^+ N K_j$ are uniformly bounded and the solution is itself bounded. Since ℓ is also bounded, it is enough to check if

$$\sum_{T} \sum_{M_i \neq M_j} \left(\varphi_i - \varphi_G^T\right) \cdot \ell\Phi_i^{\text{N}} = \mathcal{O}(h^2).$$

In fact,

$$\Phi_i^{\mathrm{N}} = \sum_{j \neq i} K_i^+ N K_j^- (\tilde{W}_i - \tilde{W}_j) = \sum_{j \neq i} K_i^+ N K_j^- \langle \widetilde{\nabla \pi_h(W)}, \mathbf{M}_i \mathbf{M}_j \rangle,$$

where $\pi_h(W)$ is the piecewise linear interpolant of W.[2] The matrices $N K_j^-$ are bounded, the matrices K_i^+ are $\mathcal{O}(h)$, and $\mathbf{M}_i \mathbf{M}_j$ is also $\mathcal{O}(h)$ if the mesh is regular. Hence $\Phi_i^{\mathrm{N}} = \mathcal{O}(h^2)$ on any triangle. Moreover, $\varphi_i - \varphi_G^T = \mathcal{O}(h)$, so it is enough to check if $\ell = \mathcal{O}(h)$. Since W is the exact solution and $\pi_h(W)$ is the piecewise linear interpolant of W, we have

$$\langle v_i, l(\Phi_i^{\mathrm{LDA}}) \rangle = \mathcal{O}(h^3) \quad \text{and} \quad \langle v_i, l(\pi \Phi_i^{\mathrm{LDA}}) \rangle = \mathcal{O}(h^3).$$

As we have seen just above,

$$\langle v_i, l(\Phi_i^{\mathrm{N}}) \rangle = \mathcal{O}(h^2) \quad \text{and} \quad \langle v_i, l(\pi \Phi_i^{\mathrm{N}}) \rangle = \mathcal{O}(h^2),$$

and thus $\ell = \mathcal{O}(h)$.

However, there is an important difference between what is done on the entropy wave and its orthogonal. On the entropy wave, the scheme can be naturally associated to a finite element method with discontinuous test functions, as with the SUPG method. This is much less clear for what we do on the orthogonal complement of the entropy wave.

ACKNOWLEDGMENTS

REFERENCES

1. R. Abgrall, On essentially non-oscillatory schemes on unstructured meshes: Analysis and implementation, *J. Comput. Phys.* **114**, 45 (1994).

2. R. Abgrall and T. J. Barth, *Linearisation via the Entropy Variables: Application to Residual Distributive Schemes*, Rapport de Recherches n⁰ 00-15 (Mathématiques Appliquees de Bordeaux, 2000), submitted for publication.

3. R. Abgrall and K. Mer, *Un théorème de type Lax–Wendroff pour les schémas distributifs*, Technical Report 98010 (Mathématiques Appliquées de Bordeaux, 1998).

4. T. J. Barth, Some working notes on the N scheme, private communication, 1997.

5. H. Deconinck, P. L. Roe, and R. Struijs, A multidimensional generalization of Roe's difference splitter for the Euler equations, *Comput. Fluids* **22**, 215 (1993).

6. H. Deconinck, R. Struijs, G. Bourgeois, and P. L. Roe, Compact advection schemes on unstructured meshes. in *24th Computational Fluid Dynamics*, VKI Lecture Series 1993-04 (von kármán. Institute, 1993).

7. A. Dervieux, B. van Leer, J. Périaux, and A. Rizzi, *Numerical Simulation of Compressible Euler Flows*, Notes on Numerical Fluid Mechanics (Vieweg, Wiesbaden, 1989), Vol. 26.

---

[2] $\mathbf{M}_i \mathbf{M}_j$ is the vector starting at point M_i and ending at point M_j.

8. L. Fezoui and B. Stoufflet, A class of implicit upwind schemes for Euler simulations with unstructured meshes, *J. Comput. Phys.* **84**, 174 (1989).

9. A. Harten, On the symmetric form of conservation laws with entropy, *J. Comput. Phys.* **49**, 151 (1983).

10. M. Y. Hussaini, B. van Leer, and J. Van Rosendal, Eds., *Upwind and High Resolution Schemes* (Springer-Verlag, Berlin/New york, 1997).

11. P. Lax and B. Wendroff, Systems of conservation laws, *Comm. Pure Appl. Math.* **13**, 381 (1960).

12. P. L. Roe and D. Sidilkover, Optimum positive linear schemes for advection in two and three dimensions, *SIAM J. Numer. Anal.* **29**(6), 1542 (1992).

13. R. Struijs, H. Deconinck, and P. L. Roe, Fluctuation splitting schemes for the 2D Euler equations, in *Computational Fluid Dynamics, 1991*, VKI Lecture Series 1991-01 (Von Kármán Institute, 1991).

14. E. Tadmor, The numerical viscosity of entropy stable schemes for systems of conservation laws, *Math. Comput.* **49**, 91 (1987).

15. E. van der Weide and H. Deconinck, Positive matrix distribution schemes for hyperbolic systems, in *Computational Fluid Dynamics 1996* (Wiley, New York, 1996), pp. 747–753.

16. O. Axelsson, *Iterative Solution Methods* (Cambridge Univ. Press, Cambridge, UK, 1996).